Optimization of the culture of Chlorella sorokiniana PA.91 by RSM: effect of temperature, light intensity, and MgAC-NPs

Article *in* Environmental Science and Pollution Research · February 2023

CITATIONS
0

READS
58

2 authors:

Masumeh Panbehkarbisheh
Babol Noshirvani University of Technology
5 PUBLICATIONS **2** CITATIONS
SEE PROFILE

Hassan a.rad
Babol Noshirvani University of Technology
25 PUBLICATIONS **230** CITATIONS
SEE PROFILE

Environmental Science and Pollution Research
https://doi.org/10.1007/s11356-023-25779-y

RESEARCH ARTICLE

Optimization of the culture of *Chlorella sorokiniana PA.91* by RSM: effect of temperature, light intensity, and MgAC-NPs

Masoumeh Panbehkar Bisheh[1] · **Hasan Amini Rad**[1]

Received: 15 September 2022 / Accepted: 30 January 2023

Abstract

The unique physicochemical properties of magnesium amino clay nanoparticles (MgAC-NPs) tends to be beneficial in the application as a co-additive in treating microalgae. Also, MgAC-NPs can create oxidative stress in the environment, concurrently elective control bacteria in mixotrophic culture, and stimulate CO_2 biofixation. The condition of the cultivation of newly isolated strains, *Chlorella sorokiniana PA.91*, was optimized for the first time for MgAC-NPs at various temperatures and light intensities in the culture medium of municipal wastewater (MWW) by central composite design in the response surface methodology (RSM-CCD). This study examined synthesized MgAC-NP with their FE-SEM, EDX, XRD, and FT-IR characteristics. The synthesized MgAC-NPs were naturally stable, cubic shaped, and within the size range of 30–60 nm. The optimization results show that at culture conditions of 20 °C, 37 µmol m^{-2} s^{-1}, and 0.05 g L^{-1}, microalga MgAC-NPs have the best growth productivity and biomass performance. Maximum dry biomass weight (55.41%), specific growth rate (30.26%), chlorophyll (81.26%), and carotenoids (35.71%) were achieved under the optimized condition. Experimental results displayed that *C.S. PA.91* has a high capacity for lipid extraction (1.36 g L^{-1}) and significant lipid efficiency (45.1%). Also, in 0.2 and 0.05 g L^{-1} of the MgAC-NPs, COD removal efficiency 91.1% and 81.34% from *C.S. PA.91* showed, respectively. These results showed the potential of *C.S. PA.91*-MgAC-NPs for nutrient removal in wastewater treatment plants and their quality as sources of biodiesel.

Keywords MgAC-NPs · Microalgae · CCD–RSM · COD removal · Lipid · Light · Temperature

Introduction

Water is one of the most critical bases in our life that needs to be conserved due to the increasing population. Industrial and human activity causes an increase in biological and chemical contaminants (Vasistha et al. 2020). By 2030, there may be a 40% water deficit (Nashmin Elyasi et al. 2021).

Conventional methods are generally used in wastewater treatment through the use of dripping filters, and efficiently activated mud eliminates organic pollutants but is not practical for inorganic problems. However, it is necessary to develop a profitable approach to treating wastewater and reach nutritional recovery (Lee et al. 2021). The advantage of using microalgae is that they grow in watery media and flat water on non-arable ground and have rapid growth, and many species have an oil amount in the dry weight range of 20 to 50% biomass, biofixation of waste CO_2, and obtained nutrients from wastewater (Sirajunnisa and Surendhiran 2016). It does not require herbicides or the application of pesticides; produces useful co-products such as protein and residue biomass after oil extraction, which can be used as feed or dung or soured to generate ethanol or methane; and are capable of biological photo production of "bio hydrogen" (de Farias Silva and Bertucco 2016; Almomani et al. 2019). Microalgae are rich in high-value compounds, for example, protein, vitamins, pigments, and active biological compounds used in cosmetics, medicines, nutraceuticals, food, and the feed industry (Liyanaarachchi et al. 2021).

Ferreira et al. studied the biotags of wastewater using microalgae and established the first algae ponding system for

Responsible Editor: Diane Purchase

✉ Hasan Amini Rad
h.a.rad@nit.ac.ir

Masoumeh Panbehkar Bisheh
m.panbehkarbisheh@nit.ac.ir

[1] Department of Environmental Engineering, Faculty of Civil Engineering, Babol Noshirvani University of Technology, Babol 47148-7313, Iran

Published online: 18 February 2023

processing city waste in 1950. Microalgae can use the abundant sunlight that falls on the surface of sewage as an energy source for growth and, at the same time, remove contaminants (nitrogen, phosphorus, pharmaceutical compounds, and pesticides, and reduction of carbon dioxide). Dairy effluents and urban wastewater are suitable culture mediums for mixtrophic microalgae and produce fat for biodiesel synthesis (Ferreira et al. 2018). Geider and Roche (2002) suggested a C:N:P ratio of 46.1:7.7:1 for algal growth, while the dairy wastewater we used in this study had a C:N ratio C:N:P ratio of 37.9:3, 0:1 (Geider and Roche 2002). Low levels of C and N compared to the recommended weight limit can positively affect biomass production since N deficiency stress can increase the lipid content of algal cells (Choi 2016). Microalgae can use nutrients left in dairy wastewater for growth. This method had the advantage of both biomass production and removal of nutrients in dairy wastewater. Carbon dioxide (CO_2) is a crucial factor that significantly improves algae biomass results. About 1 kg of dry algae biomass in open pond culture utilizes 1.83 kg of carbon dioxide (Chen et al. 2018; Cezare-gomes et al. 2019; Ubando et al. 2020). Reports are also available on reducing BOD, COD, and high levels of nitrogen compounds by algae cultures in different wastewaters (Di Caprio et al. 2019; Saranya and Shanthakumar 2020). Microalgae can be essential in producing bioenergy if integrated with wastewater remediation when growing biomass for biofuel raw materials (Ahmad et al. 2021).

Asadi et al. studied wastewater treatment from dairy using *Chlorella sorokiniana* PA.91 and Chlorella Vulgaris. They found that the optimum temperature observed for Chlorella Vulgaris and *Chlorella sorokiniana* PA.91 were 25 °C and 28 °C, respectively. The μ and productivity values of *Chlorella sorokiniana* PA.91 biomass in the effluent from the pretreatment unit were 0.375 day^{-1} and 0.233 g L^{-1} day^{-1}, respectively. They have also determined these parameters in the effluent of the secondary treatment unit 0.422 day^{-1} and 0.185 g L^{-1} day^{-1}, respectively (Asadi et al. 2019). Also, at a light intensity of 2500 lx and primary and secondary effluents, the maximum lipid content of *C. sorokiniana* PA.91 was observed to be 31% and 35%, respectively (Asadi et al. 2020). Yaqoubnejad et al. showed a significant improvement in microalgae growth (up to 61%) in the proposed hexagonal airlift flat plate (HAFP) photobioreactor. The highest CO_2 removal of 53.8% and bioremediation of 0.85 g L^{-1} day^{-1} achieved in the HAFP photobioreactor is about 70% more than that of the flat plate (TFP) photobioreactor. The results suggested that the HAFP photobioreactor could accelerate nutrient removal and achieve significantly higher efficiencies of 91%, 99%, 97%, and 93% for ammonia (NH_3), nitrate (NO_3^-), phosphate (PO_4^{-3}), and chemical oxygen of demand (COD) within seven days of cultivation (Yaqoubnejad et al. 2021). According to the studies on this native microalgae, no Nano studies have been done to optimize the culture conditions.

González-Camejo et al. studied the effects of light intensity and temperature on nutrient removal and biomass productivity in a microalgae-bacterial culture and their impact on microalgae-bacterial competition. They found that biomass production increased significantly with light intensity, reaching 50.5 ± 9.6, 80.3 ± 6.5, and 94.3 ± 7.9 mg $VSS \cdot L^{-1} \cdot day^{-1}$ for the light intensity of 40, 85, and 125 $\mu E \cdot m^{-2} \cdot s^{-1}$, respectively (González-Camejo et al. 2018). Khalili et al. investigated the effects of different nitrogen sources and nutrient concentrations in the growing medium and other LED light wavelengths and intensities on the biomass production of the green alga *Chlorella vulgaris*. Warm white light with an intensity of 80 $\mu mol/m^2/s$ was the most suitable light for biomass production, and the highest biomass concentration (1.37 g/L) was obtained (Khalili et al. 2015). Nally et al. studied the temperature's effect on the algae growth rate, biomass accumulation, production, and fatty acid composition. They surveyed 26 algal species from 5 different functional groups, growing them at six different temperatures between 9 and 32 °C. Temperature responses varied between species, but at the functional group level, we found that cyanobacteria have the highest thermal optimum (30.6 ± 2.3 °C), followed by chlorophytes (25.7 ± 0.1 °C) and diatoms (24.0 ± 0.4 °C). In general, the temperature significantly affects the overall productivity of algal biomass systems by influencing species growth rates and fatty acid production (Nalley et al. 2018). Carneiro et al. (2020) investigated the effects of temperature on biomass production, nighttime biomass loss, and photosynthetic changes using *Nanochloropsis oceanica* as a model species in two outdoor 50-L tubular photobioreactors (PBR) and revealed increases in these parameters. Cultures were exposed to daily light in two independent experiments: a dark cycle at a constant temperature of 28 °C and another at 18 °C. As a result, *N. oceanica* exhibited wide temperature tolerance with significant nocturnal biomass loss. This will remove crystals at lower temperatures, with a loss of productivity each day (Carneiro et al. 2020).

Nanoscience is one of the most important borders and the development of research in modern science. Nanoparticles (NPs) offer many advantages because of their unique physical size and nature. Because of the extensive NP application in biomedical, biotechnology, engineering, material science, and environmental fields, much attention has been given to preparing for various types of NP (Singh et al. 2018). Several studies have shown that nanoparticles (NP) have broad ability and potential in wastewater treatment, especially with the help of adsorption and facilitate the breakdown of contaminants (Vasistha et al. 2020). Some nanomaterials comprising TiO_2, manganese oxide, carbon nanotubes, and ZnO have proven influential roles in the oxidizing of contaminants due to their

large surface area and fast adsorption capacity (Naseem and Waseem 2021).

MgAC-NPs are attractive among other nanoparticles due to promote the growth of microalgae due to the action of propylamine, its composition, and variation in water (Khac et al. 2018). Several studies have used MgAC-NPs to improve microalgae culture, harvesting, recovery, and lipid production. (Farooq et al. 2016; Kim et al. 2016, 2020; Nguyen et al. 2019). Y. Lee et al. show that Chlorella sp. KR-1 (1.7 g L^{-1} of biomass) was harvested 30 min after the injection of MgAC-NPs at concentrations above 0.6 g L^{-1} at constant pH (Lee et al. 2014). Also, MgAC-NPs affected an increase in cell size (3,524–4,175 µm) with low cell density, and the total rise in lipid levels without change of microalgae cells is under different doses of MgAC-NPs (0, 25, 0.5, and 1 g L^{-1}) in the layer of 2.0% CO_2 (Farooq et al. 2016). Adding 0.01–0.1 g L^{-1} MgAC-NP promoted microalgae biomass production above lower control through differential biocide properties on microalgae cells and bacteria (Kim et al. 2016). In the attendance of MgAC-NPs at contents ranging from 0 to 0.1 g L^{-1}, SP KW microscopically cells' growth has increased more than the non-MgAC cases. Even at this low concentration, MgAC-NPs can grow microalgae metabolic accumulation (Kim et al. 2020).

However, the specific objectives of this work are to (i) to investigate optimal conditions for C. S PA.91 growth with microalgae cultivation in MgAC-NP, variable temperatures, and light intensity in wastewater culture media through design expert-13 (RSM–CCD) software; (ii) possibility cultivate microalgae using real municipal wastewater in optimal culture conditions; (iii) Studying the performance of *C.S. PA.91* comprehensively for lipid extraction and city wastewater treatment. To do this, C.S. PA.91 was cultivated in a 250-mL Erlenmeyer flask with a 200 mL work volume using municipal wastewater under optimum culture conditions. Finally, this study provides an effective strategy for MgAC-NPs and wastewater treatment by a new strain. Overall, this research can be classified in the "Microalgae Research System" based on "cell milking", which provides an effective strategy for lipid extraction and wastewater treatment using novel strains possessing MgAC-NPs that have not been studied before. Furthermore, the current hypothesized process can pave the way for futuristic endeavors to conjugate nanoparticles and microalgae for viable and commercial production of biofuel, nanoparticles, and many other molecules.

Materials and methods

MgAC-based C.S. PA.91 cultivation and growth media

C.S. PA.91 was isolated locally from Gela Dairy Wastewater Treatment Plant (Asadi et al. 2019) and used throughout this study. One colony of *C.S. PA.91* was cultured in BG-11 medium and was added to a 250-mL autoclaved Erlenmeyer flask containing 100 mL of BG-11 medium within a shaker with interior environmental conditions (28 °C; 100 rpm; light intensity 46.25 µmol m^{-2} s^{-1}) at 12:12 light/dark cycles for 15 days. Reducing fat oil grease and suspended particles could have hampered the efficiency of wastewater as a culture medium, taking the culture media from the influent to the primary settlement tank of the urban wastewater treatment plant (WWTP). This experimental study was used in Sari, Iran (Table 1). In this research, three different cultures, such as BG-11, autoclaved, and raw wastewater, were used, and their performances were predicted and experimentally achieved. To avoid competition for consumption of nutrients between the symbiotic relationship between bacteria and microalgae cells, wastewater samples were autoclaved at 120 °C for 20 min and then held at 4 °C.

In the present experimental study, a sample of *C.S. PA.91* was used to prepare the culture medium in a liquid medium and Erlenmeyer 250 mL with a working volume of 200 mL and inside an incubator shaker (at a temperature of 28 °C and 120 rpm and also the light intensity on the surface of the Erlenmeyer by an average lamp of 2800 lx (51.8 molµ photons m^{-2} s^{-1}). The effect of different concentrations of MgAC-NPs on the growth of *C.S. PA.91* was experimentally investigated in wastewater (pH 7.8) culture under light–dark conditions for 12–12 h in wastewater.

Analytical methods

In this section, first, the growth analysis is determined. Then, the materials, equipment, studied cultural states, and media are described. Also, the methods for calculating the amount of microalgae biomass; resolving the specific growth rate, chlorophyll, and carotenoid concentration; and synthesizing magnesium-amino clay (MgAC) are present. Also, the statistical analysis described is the optimization of the microalgae

Table 1 Specifications of the wastewater media accustomed in this study

Parameter	Units	Entrance to the treatment plant	Preliminarily treated effluent	Secondary treated effluent
TSS	mg L^{-1}	275	102	60
BOD_5	mg L^{-1}	205	136	79.38
COD	mg L^{-1}	410	272	141.69
TN	mg L^{-1}	25	35	10
TP	mg L^{-1}	3	3	1.5
pH	–	7.8	7.8	8.1
$N\text{-}NO_3^-$	mg L^{-1}	12	12	7
$N\text{-}NH_4^+$	mgL^{-1}	13	13	2
Turbidity	FAU	112	102	7.6

growth utilizing response surface methodology–central composite design (RSM–CCD) determination of lipid. Eventually, the methods of measuring the nitrate, ammonia, phosphate, and chemical oxygen demand (COD) are described. The COD analysis was carried out by the protocol characterized by the American Public Health Association (Baird et al. 2017) using a digester (COD Hatch reactor) and colorimeter (direct spectrophotometer of Hatch Dr./2000) at a wavelength of 600 nm. The percentage of COD decrease is computed with the Eq. (1), where cod_i is the request of initial chemical oxygen and cod_f is final. COD is measured via time. Information was gathered in the temple.

$$\text{COD removal}(\%) = (\text{COD}_i - \text{COD}_f)/\text{COD}_i \times 100 \quad (1)$$

Growth analysis

The cell's dry weight is measured using optical density at 680 nm (OD_{680}) in a UV–Vis spectrophotometer (UNICCO 2800 UV-seen, 4 nm, 110 V, China). In this experiment, 2 mL of culture was centrifuged in the stationary phase utilizing a resolved corner centrifuge (Centrifuge RST-24, Yarran Tajhiz Iran) at 4000 rpm for 15 min. The biomass concentration was calculated by the cell dry weight method (CDW), in which a sample of microalgae cells was washed and dried in an oven at 70 °C every 24 h. The standard curve has schemed with OD_{680} in various microalgae biomass concentration ranges (Asadi et al. 2020). Biomass concentration (CDW, g L^{-1}) and specific growth (μ, d^{-1}) rates are calculated using Eqs. (2) and (3): (Yaqoubnejad et al. 2021).

$$\text{CDW} = 1.824\text{OD}_{680} + 0.043, \left(R^2 = 0.9889\right) \quad (2)$$

$$\mu = \ln\left(C_f/C_0\right)/(t_f - t_0) \quad (3)$$

OD_{680}, C_f, and C_0 were expressed as optical density at 680 nm, final and initial biomass concentration (g L^{-1}), and time; t_f and t_0 showed final and initial times of the cell growth phase (day), respectively.

Measurement of chlorophyll and carotenoid concentration

In this study was used the modified Becker method to measure chlorophyll and carotenoid from the supernatant of a 5-mL sample of microalgae centrifuged at 3000 rpm for 15 min (Das and Sahoo 2019). The pellets were washed twice, suspending 5 mL of clarified water, and centrifuged at 3000 rpm for 10 min. Supernatants were discarded, 3 mL 90% methanol added, and vortexed for 5 min to blend. Samples were incubated in a water bath of 60 °C for 60 min. Selections were then constructed to 5 mL with 90% methanol and centrifuged at 3000 rpm for 15 min. The supernatant is accumulated in a clean reaction tube and is used to read absorbance reading.

Extracts were diluted with clarified water, and the absorbance was measured at 470, 650, 655, and 750 nm using a UV–visible spectrophotometer (UNICCO 2800 UV–Visible, 4 nm, 110 V, China). Chlorophyll and total carotenoid contents were computed using Eqs. (4), (5), and (6) (Ogbonna et al. 2021):

$$\text{Chla}\left(\mu\text{gmL}^{-1}\right) = 16.72A_{660} - 9.16A_{650} \quad (4)$$

$$\text{Chlb}\left(\mu\text{gmL}^{-1}\right) = 34.09A_{650} - 15.28A_{660} \quad (5)$$

$$\text{Carotenoid}\left(\mu\text{gmL}^{-1}\right) = \left(1000A_{470} - 1.63\text{Chla} - 104.9\text{Chlb}\right)/221 \quad (6)$$

Synthesis of MgAC-NPs

MgAC-NP used in this research was prepared by a modified sol–gel method using 3-aminopropyltriethoxysilane (APTES) according to the manufacturing protocol (Farooq et al. 2016). In brief, the admixture containing $MgCl_2$●$6H_2O$ (8.4 g) and ethanol (200 mL) was dissolved in distilled water. After 10 min of magnetic stirring, APTES (13 mL) was transferred to the solution and stirred overnight. The white-slurry MgAC-NPs were formed and centrifuged at 3000 rpm for 15 min. The sediment of the solution (MgAC-NPs) was separated and washed twice with 100 mL of ethanol solution. Hence, it dried in the oven at 60 °C, and eventually, MgAC-NPs in the form of pebble powder were ground. Finally, 10 mg mL^{-1} of MgAC-NPs was placed in a 100-mL plastic bottle to confirm the delineation of the MgAC-NPs in an aqueous solution; it is shower-sonicated for 5 min, showing the appearance of being dissolved and transparent.

Characterization of magnesium-aminoclay (MgAC)

The morphological character of produced MgAC-NPs was determined using a scanning electron microscope (FE-SEM) and elemental analysis (EDX) using TESCANS 9000, which operates in 10 kV acceleration voltage, which showed the elements of the samples and confirmed the characteristics of the example. The crystalline structure of the MgAC-NPs was determined by XRD X-ray diffraction (GNR Srl, Italy, Explorer, Cu-Kα radiation). The diffract grams were recorded in the range 2θ from 10 to 80° with a 0.01° step size and a sweep time of 1 s step by step. Fourier transformation infrared spectroscopy (FT-IR, Thermo, Avatar, USA) from 4000 to 400 cm^{-1} was used to predict the structural and chemical bond (targeting functional groups).

Optimization of the C.S. PA.91 growth using RSM–CCD

In this research, the RSM-CCD method was utilized initially to forecast the model, optimize these conditions' cultivation, and assess the considerable effect of aquaculture conditions on biomass results. A statistical analysis of the univariate variance has been established to find essential factors and the effect of their interaction in response to microalgae growth. Also, the three-dimensional surface layout (3D) and the appropriate contour plot obtained from the mathematical model explain each factor and its interactions' effects on the response. Eventually, the optimal area of each was uncertain (in the range), where maximum biomass results are predicted to use optimization and numerical desires. Numerical optimization of the cultivation condition is done by regulating the input uncertain X_1, X_2, and X_3 in the various levels and maximizing the response. The number of answers produced and the points or areas that maximize the desired function are considered an optimized growth condition for microalgae.

The growth optimization of *C.S. PA.91* with and without MgAC-NPs was determined in a 250-mL Erlenmeyer flask with a working volume of 200 mL under different light, intensity, temperature, and MgAC-NP concentration. Study of optimization culture conditions to the executed through design expert-13 (RSM–CCD) software and composition of mathematical and statistical techniques to assess the significant relative factors of cell cellular weight (CDW), growth rate (μ), chlorophyll, and carotenoid. All experimental processes are carried out in triplicates for 15 days for each run in several cultivation situations, such as the concentration of MgAC-NP in different contents, the intensity of the light, and the temperature suggested in Table 2.

The conditions selected for this study were based on existing data (Asadi et al. 2019; Yaqoubnejad et al. 2021) and replicating experiments. Finally, optimized growth conditions experimentally measured cell dry weight (CDW), growth rate (μ), chlorophyll, and carotenoid contents. Experiments are carried out with 20 runs for the selected factors to meet the CCD. The results of the optimization system fit a cubic model by the ANOVA to characterize the interaction between free and dependent factors. As a result, with a general expression as displayed in Eq. (7):

$$y = \beta_0 + \sum_{i=1}^{k} \beta_i x_i + \sum_{i=1}^{k} \beta_{ii} x_i^2 + \sum_{1 \le i \le j}^{k} \beta_{ij} x_i x_j + \varepsilon \quad (7)$$

where y is a response (dry cell weight (DCW), growth rate (μ), chlorophyll and carotenoid content); x_i, x_j, …., x_k is input factor (light, temperature, and MgAC concentration); β_0 is the term interceptor; β_i ($i = 1, 2, \ldots, k$) is a linear effect, β_{ii} ($i = 1, 2, \ldots, k$) is a squared effect, and β_{ij} ($i = 1, 2, \ldots, K$, $J = 1, 2, \ldots, K$) is an effect of interaction. The R^2 correlation coefficient verified the credit of the equation by the second-order model. R^2 value closer to 1 indicates a good communication between the empirical results and the model's prediction.

Determination of lipid

Lipid is determined by using the sulfo-phospho-vanillin (SPV) reagent. SPV is made by dissolving 0.6 g of vanillin in 10 mL of sheer ethanol and then 90 mL of water deionization (Mishra et al. 2014). In addition, 400 mL H_3PO_4 is concentrated and added to the admixture and stores the reagents produced in dark bottles in room conditions. 2.0 mL of H_2SO_4 concentrated (98%) to measure microalgae lipids was added to lipid microalgae samples, heated for 10 min at 100 °C, and then kept for 5 min in ice baths. Five milliliters of the newly ready SPV reagent was added, and samples were incubated for 15 min at 37 °C in the incubator shaker (200 rpm); the spectrophotometer visible UV at a 530 nm lipid concentration in a microalgae lipid sample is measured. Lipid production and content were defined by Eqs. (8) and (9):

$$\text{Lipid production}\left(\text{gL}^{-1}\right) = \text{lipid(g)}/\text{volume(L)} \quad (8)$$

$$\text{Lipid content}(\%) = \text{lipid(g)}/\text{mass of culture(g)} \times 100 \quad (9)$$

Standard curve for the determination of lipids by SPV

The standard lipid stock is prepared using 2 mg commercial canola oil in chloroform 1 mL^{-1}, which has been kept in a fresh box at – 4 °C before being used (Fig. S1). The different concentrations of lipids in the standard oil solution have been added to the clean tube. The tube was maintained in hydroceles at 60 °C for 10 min to vaporize the

Table 2 Coded factors and levels for optimal microalgae growth

Factors		Coded factor levels				
		$-\alpha$	−1	0	+1	$+\alpha$
Temperature (°C)	X_1	15	20	25	30	35
Light intensity (μ mol m^{-2} s^{-1})	X_2	1000	2000	3000	4000	5000
MgAC (g L^{-1})	X_3	0	0.05	0.1	0.15	0.2

solvent, and 100 µL of water was eked to the lipid standard (Visnovitz et al. 2019). Other samples have been provided and defined according to Park et al. (2016) by the SPV reaction method explained previously (Park et al. 2016).

Statistical analysis

In this research, RSM-CCD was initially used to predict the model, optimize the cultivation condition, and designate the significant effects of cultivation conditions on biomass results. The correlation between *C.S. PA.91* growth rates and pigment contents is defined using bivariate analysis. In this research, RSM-CCD was initially utilized to predict the model, optimize the cultivation condition, and assess the meaningful effects of cultivation conditions on biomass results. Based on the correlation results, multifold regression analysis measures numerical associations between microalgae growth rates and pigment content. Because bivariate analysis shows a strong solidarity between microalgae growth responses and pigment content, the significant effect of cultivation conditions on microalgae growth responses and analyzed pigment content was determined using multiple analyses of variance (MANOVA), where P values < 0.05 (Fig S2). Furthermore, the univariate variant (ANOVA) analysis between the cultivation condition and the percentage of accumulation of lipids is carried out to determine a meaningful cultivation condition for lipid production in microalgae. The development of microalgae must be considered as large-scale systems, such as wastewater treatment, MgAC-NP performance based on natural wastewater rather than artificial was evaluated and the COD reduction percentage under different operating conditions of adding MgAC-NPs by the native *C.S. PA.91* microalgae of wastewater was assessed.

Results and discussion

Characterization of the MgAC-NPs

The initial characterization of MgAC-NPs was performed to determine its particle size and purity before being utilized. FE-SEM image of the inorganic–organic MgAC powder is shown in Fig. 1a, where the spherical or ellipsoidal nano clay with a smooth surface was observed in the agglomerated state and polydispersed 30–60 nm size ranges. Figure 1b illustrates the estimated structure of the MgAC unit (chemical composition: $[H_2N(CH_2)_3]_8SI_8MG_6O_{12}(OH)_4$) (Farooq et al. 2016), and also shows if the structure of the produced MgAC-NPs is rudimental.

An octahedral brucite sheet ($Mg(OH_2)$) is in the middle and is flanked between the silica tetrahedral sheet, so it forms phyllosilicate Smectite 2:1. In silica tetrahedral, organic pendant $-(CH_2)_3NH_2$ is very crowded. SEM–EDX analyzes MgAC-NPs to evaluate the morphology of the surface and the percentage of atoms. Figure 2 displays the EDX spectrum of MgAC-NPs synthesized nanoparticles. The composition of nanoclay was performed by EDX and the element in the nano clay framework was tracked. The maximum intense point obtained from the EDX spectra is Mg and Si. The elemental profile of MgAC-NPs confirmed the elemental Mg and Si signals at 1.35 and 1.98 keV, respectively. The fundamental analysis revealed that oxygen was in the highest proportion (27.74%), followed by nitrogen (15.68%) and silicon (13.93%) in nanoparticle mass (Table 3). Additional peaks for oxygen are caused by oxygen adsorbed or oxidation of particles faced, and the application of chlorine causes the rise of chlorine during the synthesis process. Similar elemental composition of MgAC-NPs is observed by Wang et al. (2017) and Li et al. (2019).

The powder x-ray diffraction (XRD) to confirm the crystal or amorphous structure of the synthesized MgAC-NPs

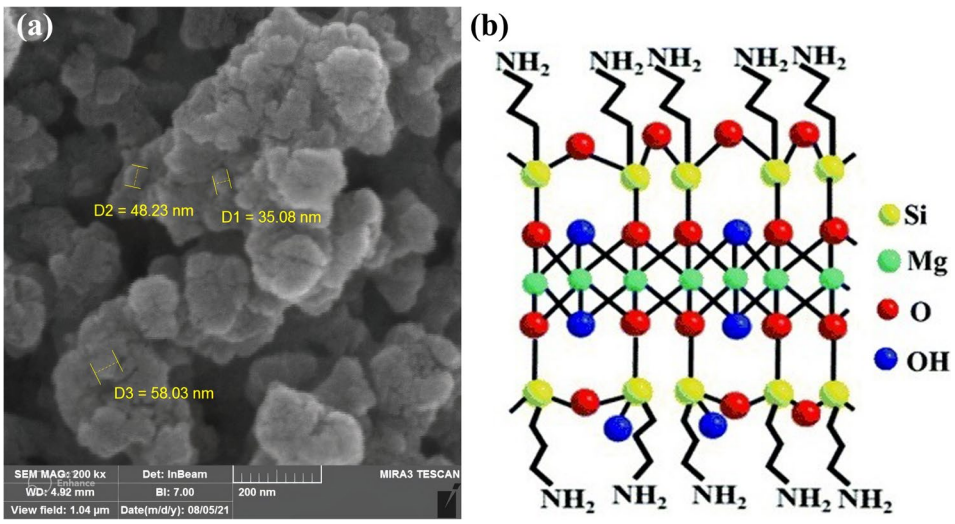

Fig. 1 **a** FE-SEM image of MgAC-NPs. **b** Two-dimensional structure of MgAC-NPs

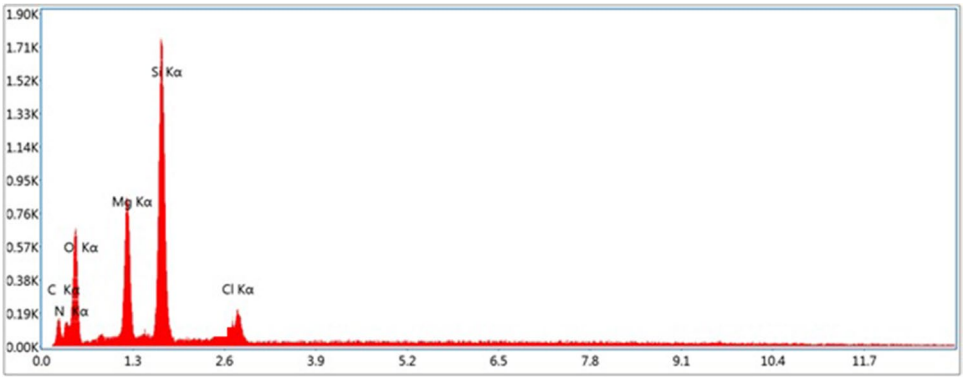

Fig. 2 EDX spectrum of MgAC-NPs

Table 3 Chemical composition of synthesized MgAC-NPs obtained through EDX

Element	Weight (%)	Atomic weight (%)
C	13.9	21.31
N	15.68	20.62
O	27.74	31.93
Mg	8.73	6.62
Si	13.93	9.13
Cl	10.01	4.4

is obtained and checked (Fig. 3). A typical propeller structure with an actual distance is consistent with an inosculate organic amino propyl lug. Furthermore, the reaction in a broad field at a higher angle ($d_{020,110} = 0.41$ nm; $d_{130,200} = 0.238$ nm) and the characteristic reaction ($d_{060,330} = 0.157$ nm) in 2θ confirm the formation of mg-phyllosilicate trioctahedral clay 2:1 with a structure such as powder (Lee et al. 2014; Ji et al. 2016; Fu et al. 2017; Bui et al. 2018; Li et al. 2019). Therefore, we can conclude that the organizational framework for MgAC-NPs is characterized as a structure of silicate amino propyl tied along the two sides of the coordinate bonds octahedron MgO/OH on brucite sheets during the starting process, and this result shows the success of biomolecules becoming MgAC-NPs.

In FT-IR analysis, the information obtained from infrared absorption is displayed as a spectrum. Surface functional properties of MgAC-NPs were analyzed using FT-IR. The broad peaks representing pure MgAC-NPs were observed at 1125 cm^{-1}, 3407 cm^{-1}, 566.32 cm^{-1}, 3034.48 cm^{-1}, 3428.71 cm^{-1}, 855.95 cm^{-1}, 790.72 cm^{-1}, 1045.84 cm^{-1}, 939.08 cm^{-1}, and 2021.73 cm^{-1} corresponding to Si–C, N–H, Mg–O, C–H_2, O–H, Mg–O–Si, Si–O–C, Si–OH, Si–O–Si, and N–H bond vibration of MgAC-NPs respectively (Fig. 4). These results showed that functional groups present in MgAC-NPs had syntheses successfully. Based on the detected peaks and their comparison with the standard peaks presented in Fig. 4b, it can be concluded that there are organic compounds in the synthesized structures. According to Si–C, N–H, and N–H_3 functional groups, aminopropyl combinations have a covalent bond. Also, the functional groups Si–O–Si, Mg–O, and Mg–O–Si indicate the phyllosilicate structure of magnesium aminoclay nanomaterial. According to the functional groups, the microalgae receives part of the micronutrients it needs using the MgAC-NPs. Similar findings were reported from Hoseini et al. (2017), Lv et al. (2018), and Li et al. (2019).

According to the functional groups identified in FT-IR analysis and comparing the results with other researchers, the synthesized MgAC-NPs have been synthesized well, and have a better positive effect on microalgae as an additive. The N:P ratio is responsible for microalgae cell proliferation that must range from 8 to 45 (Ramlee et al. 2021). In this regard, the N:P ratio in WW was found to be 8.33:1, and the ratio found suitable in media performed better concerning cell proliferation. According to Si–C, N–H, and N–H_3 functional groups, as aminopropyl combinations, also the above dissolving of MgAC-NPs as co-additive in wastewater, and the N:P ratio will increase. Finally, absorbing nutrients lead to a higher growth of microalgae, and helps in removing nutrients from wastewater.

Optimized cultivation conditions (growth rate and pigments)

The biomass replies, dry weight of cells, growth rates, chlorophyll, and carotenoid amounts, were obtained for microalgae under different empirical design conditions (Table S2). Variables of multiple processes and the best-related regions for *C.S PA.91* Investigate optimal growth of biomass utilizing the RSM-CCD method. Responses were analyzed to consider quadratic or cubic model fit. The results strongly recommended the cubic polynomial equation (in terms of fundamental factors) to express the relationship between the selected input variables (or factors), as in Table 4. The answers are studied to adapt the cubic model. The results highly recommend the cubic polynomial equation as a model to express the relationship

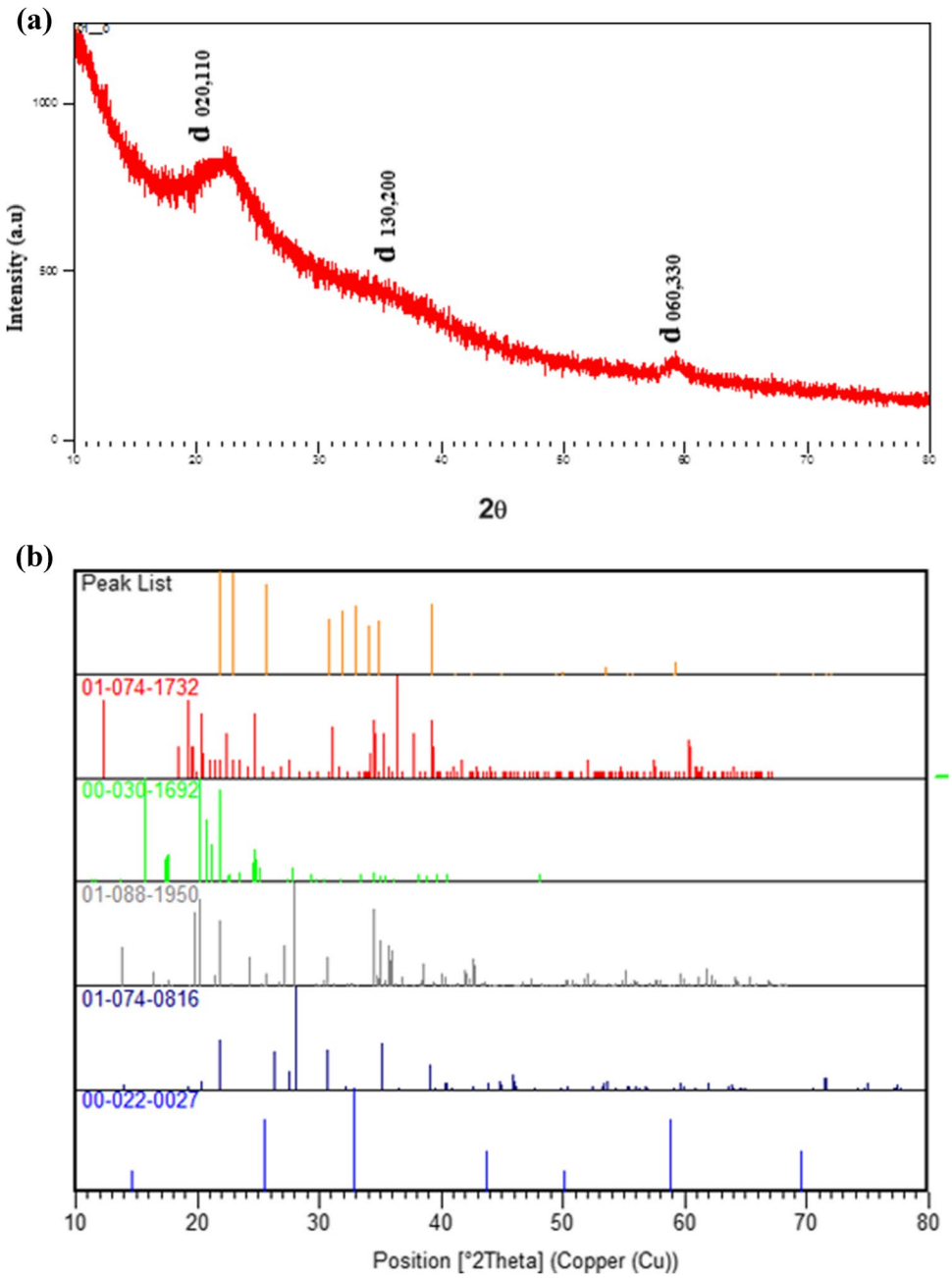

Fig. 3 XRD spectra of MgAC. **a** Detected structure; **b** detected phases

between the selected agents and replies in durations of essential elements, as presented in Table 4. Finally, the analysis of variance (ANOVA) is performed to determine the interests of the model, and the answers are publicized in a complement (Table S3-S6). Related P dependent with every model shows that the cubic model is statistically substantial in divination on the response according to fundamental factors. Also, the particularities of model analysis (predictive attention, smash ratio, and residual estimation) are complementary.

Optimized culture conditions and accurate biomass results (real and predictable) are received from the RSM-CCD model reported in Table S1. Also, RSM-CCD expands the cubic model for optimized growth conditions in Table 4. The results showed that the *C.S. PA.91* had shown maximum cell dry weight, growth rate, chlorophyll, and carotenoid at intended culture conditions ($X_1 = 74$ µmol m^{-2} $s^{-}1$, $X_2 = 20$ ℃, $X_3 = 0.05$ g L^{-1}). While C.S PA.91 has shown an optimal response to conditions ($X_1 = 37$ µmol m^{-2} s^{-1}, $X_2 = 20$ ℃, $X_3 = 0.05$ g L^{-1}). This can be done well in the temperature range between 20 ℃ to 35 ℃ and develops up to 40 ℃ contrast with microalgae (Nawkarkar et al. 2019). High temperatures lead to high metabolic growth rates, high ammonium toxicity, greater sensitivity of microorganisms to

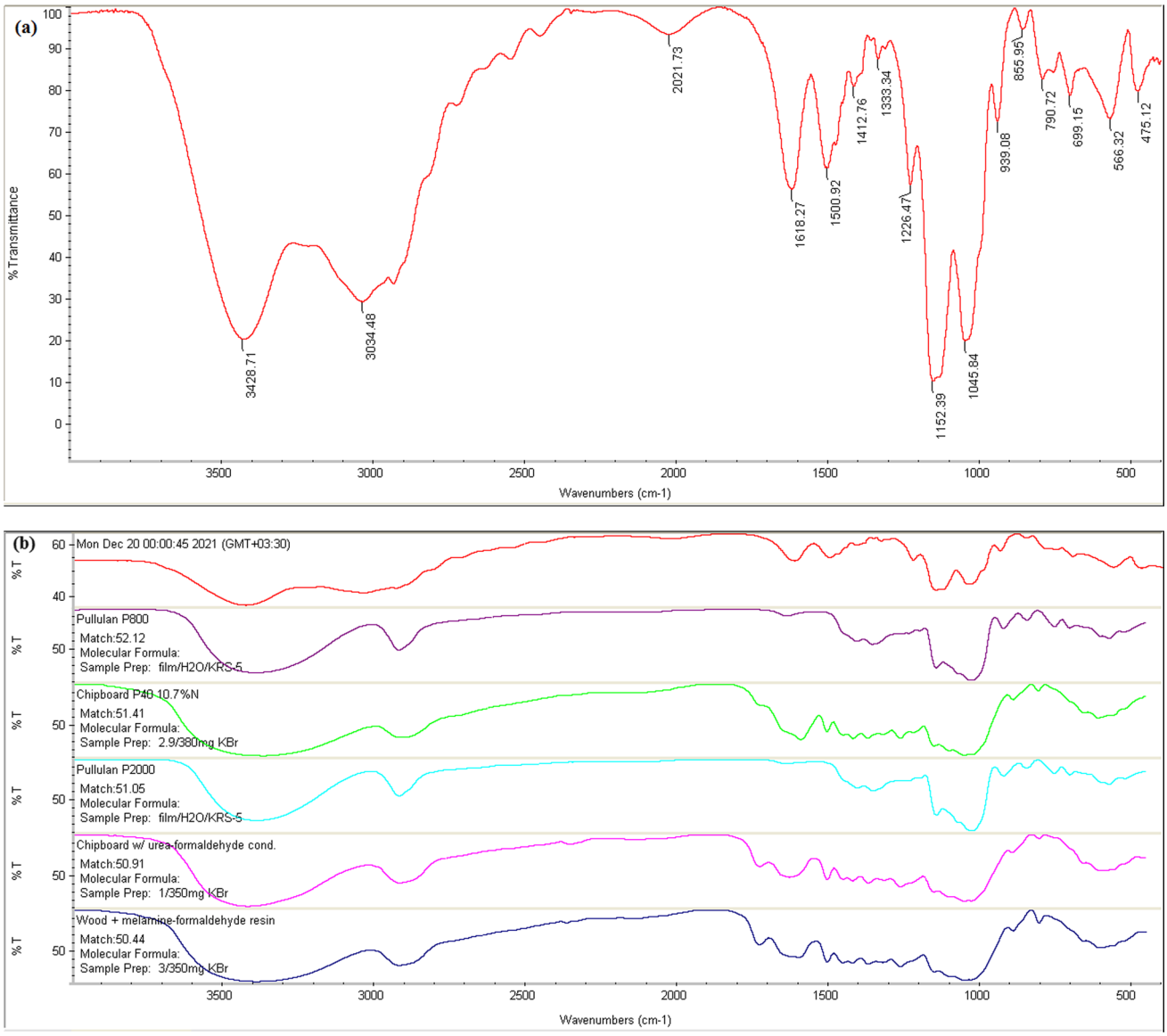

Fig. 4 FT-IR analysis of MgAC-NPs. **a** Peaks detected in nanomaterial spectrum, **b** possible organic matter based on spectrum standards and peaks

temperature changes, and foam and odor problems (Ganesh Saratale et al. 2018). In the temperature range upper 40 °C the growth and thermodynamic properties such as the shape, size, and surface morphology are different (Xue et al. 2020). Increasing temperature drastically changes the value of activation energy, which is the minimum energy entailed for the growth of microalgae (Ahmad et al. 2020). As the specific growth rate shows the compliance of microalgae to the provided environmental conditions, a relationship between the functional outcomes of MgAC NPs, microalgae growth, and pigment production is found in all empirical processes designed. The results showed that the results of microalgae biomass are powerfully associated with the specific growth rate (R value coefficient > 0.96), as presented in Fig. S3(a).

Therefore, the details of this specific growth rate can be practical when recognizing the indirect effect of cultivation conditions at the level of nutrition of wastewater. *C.S. PA.91* growth response (as cell dry weight) obtained during 20 days at optimized microalgae growth is shown in Fig. S3(b).

Where *C.S PA.91* has pursued the same propensity in wastewater culture with 3 growth term phases such as the primary lag phase, exponential growth phase (deposited), and eventually, the stationary phase for the growth of microalgae results.

C.S. PA.91 reached a residence stage in 14 days with a high CDW performance of 0.281 mg L^{-1} due to its ability to add and assimilate nutrients in wastewater when RSM-CCD

Table 4 RSM-CCD expands the cubic model for optimized growth conditions

Optimized growth condition	Response	Cubic model	*F* value	*P* value	R^2 value	Adeq precision
X_1: 2000 lx (37 µmol m^{-2} s^{-1})	DW = 0.314 mg mL^{-1}	$DW = 0.4545 + 0.0378 \times X_1 + 0.0138 \times X_2 + 0.0839X_3 - 0.0156\ X_1 \times X_2 - 0.0147\ X_1 \times X_3 + 0.0081\ X_2 \times X_3 - 0.0126\ {X_1}^2 - 0.0235{X_2}^2 - 0.0257{X_3}^2 + 0.036X_1X_2 \times X_3 + 0.0228{X_1}^2 \times X_2 - 0.1167{X_1}^2 \times X_3 - 0.0152\ X_1 \times {X_2}^2$	12.81	0.0025	0.965	14.21
X_2: 20^{0C}	μ= 0.152 day^{-1}	$\mu = 0.1801 + 0.0072 \times X_1 + 0.0029 \times X_2 + 0.0201X_3 - 0.0026\ X_1 \times X_2 - 0.0028\ X_1 \times X_3 + 0.0015\ X_2 \times X_3 - 0.0023\ {X_1}^2 - 0.0041{X_2}^2 - 0.0072{X_3}^2 + 0.0064X_1 \times X2 \times X_3 + 0.0041\ {X_1}^2 \times X_2 - 0.0256\ {X_1}^2 \times X_3 - 0.0033X_1 \times {X_2}^2$	9.13	0.0063	0.951	13.05
X_3: 0.05 g L^{-1}	Ch = 1.854 µg mL^{-1}	$Chlorophyll = 2.37 + 0.2375 \times X_1 + 0.0497 \times X_2 + 0.636\ X_3 - 0.1629\ X_1 \times X_2 - 0.0736\ X_1 \times X_3 - 0.0114\ X_2 \times X_3 + 0.0423{X_1}^2 + 0.0102{X_2}^2 - 0.1478{X_3}^2 + 0.1183X_1 \times X_2 \times X_3 + 0.0612{X_1}^2 \times X_2 - 0.8197{X_1}^2 \times X_3 - 0.0776\ X_1 \times {X_2}^2$	6.50	0.0153	0.933	12.06
	Car = 0.425 µg mL^{-1}	$Carotenoid = 0.8222 - 0.0589 \times X_1 - 0.1146 \times X_2 + 0.1037\ X_3 - 0.028\ X_1 \times X_2 + 0.0594\ X_1 \times X_3 + 0.0606\ X_2 \times X_3 - 0.0539\ {X_1}^2 - 0.037\ {X_2}^2 - 0.0924\ {X_3}^2 + 0.0436\ X_1 \times X_2 \times X_3 + 0.0727\ {X_1}^2 \times X_2 - 0.0819\ {X_1}^2 \times X_3 + 0.0354\ X_1 \times {X_2}^2$	60.93	< 0.0001	0.992	24.08

was adopted for efficient use and declared improvement actions and results in cultural conditions. Moreover, according to Table 5, X_1, X_2, X_3, and X_1X_2, X_1X_3, X_2X_3 interaction term and squared variables ${X_1}^2$, ${X_2}^2$, and ${X_3}^2$ were significant models. The lack-of-fit of R_1 (0.0048), R_2 (0.0003), R_3 (0.3811), and R_4 (0.0096) implies that the lack of compliance is significant.

Notable factors and their interplay effects on C.S. PA.91

Statistics ANOVA (*F* value and *P* value) is received in input variables, and response results have shown that light intensity (X_1), temperature (X_2), and the concentration of MgAC-NPs (X_3) have a significant influence on biomass results individually. In comparison, the intensity of light has an interaction effect with temperature (X_1X_2) and the concentration of MgAC-NPs (X_1X_3) on the dry weight of cells, growth rates, chlorophyll, and carotenoids. The surface plot of the response produced from the model has been employed for more insight into input factors' impact on the answer results. The 3D surface plot for autonomous enhancement factors (X_1–X_3) and the appropriate responses (y) are imputed in Figs. 5, 6, 7, and 8a–c.

In other words, this result means a percentage MgAC-NPs is the most significant factor impacting the meliorated dry weight of cells and growth rate amounts via microalgae cultivation. We increased the dose of MgAC-NPs from 0.05 to 0.15 g L^{-1} at a constant radiation intensity of 55.5 µmol m^{-2} s^{-1} and temperature 25 °C, CDW increased from 0.344 to 0.512 mg mL^{-1} and from 0.152 to 0.192 day^{-1}, and chlorophyll and carotenoids content rose from 1.586 to 2.855 µg mL^{-1}, from 0.626 to 0.834 µg mL^{-1}, respectively. In other words, it increased by CDW (32.8%), (20.83%), chlorophyll (44.4%), and carotenoid (24.94%). While under

Table 5 Fit statistics results obtained for the CCD-RSM of MgAC-NPs' effect

Variable	R_1 (CDW)	R_2 (growth rate)	R_3 (chlorophyll)	R_4 (carotenoid)
Standard deviation (SD)	0.0282	0.0074	0.2520	0.0399
Mean	0.4050	0.1692	2.29	0.6755
Coefficient of variation (CV%)	6.97	4.35	10.98	5.91
R^2	0.9652	0.9519	0.9337	0.9925
R^2 adjusted	0.8899	0.8477	0.7899	0.9762
R^2 prediction	− 6.1423	− 8.8797	− 12.6244	− 0.5442
Adeq. precision	14.2161	13.0522	12.0638	24.0866

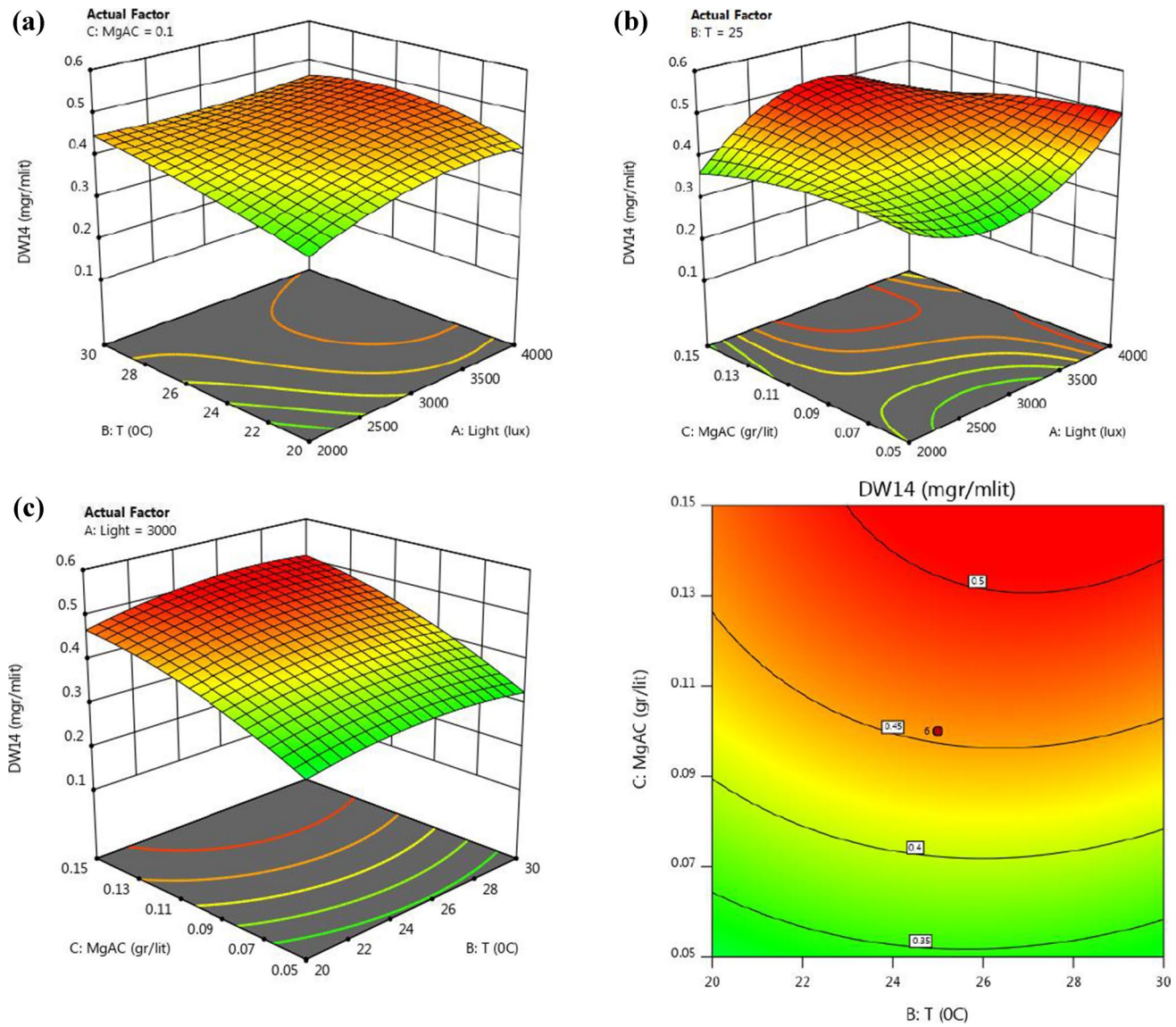

Fig. 5 Surface response scheme (3D)—considerable interaction between input changings and cell dry weight responses for *C.S. PA.91*. **a** interaction between light intensity and temperature; **b** interaction between light intensity and MgAC-NPs; **c** Interaction between temperature and MgAC-NPs on CDW responses

the same conditions, CDW (15.7%), (12.65%), chlorophyll (36.74%), and carotenoid (15.82%) were observed under the intensity of radiation and CDW (6%), (3.35%), chlorophyll (4.07%), and carotenoid (34.18%) under the influence of temperature. The lighter the medium's intensity and temperature, the higher the recovered dry weight of cells and growth rate amounts will be. The cultivation period is also essential; the recovered chlorophyll amounts increase with the cultivation time. However, in a community with a percentage of light intensity, temperature, and MgAC-NPs, the interaction factor represents a more critical and positive influence on growth. That means that an increase in the soft power and temperature with the MgAC-NPs increases the recovered dry weight of cells, growth rates, and chlorophyll amounts. ANOVA also showed that the model represents the relationship between the parameters, giving a high coefficient of designation ($R^2 = 93\%$).

Light intensity

The intensity of light changes with the turn of day and night in natural conditions (Ruan et al. 2021). Light requirements depend on species and are necessary for holding lipid synthesis. Overall, the light will obtain cell growth, biosynthesis of fatty acids, and formation of chloroplast membranes (Geada et al. 2019). In the case of

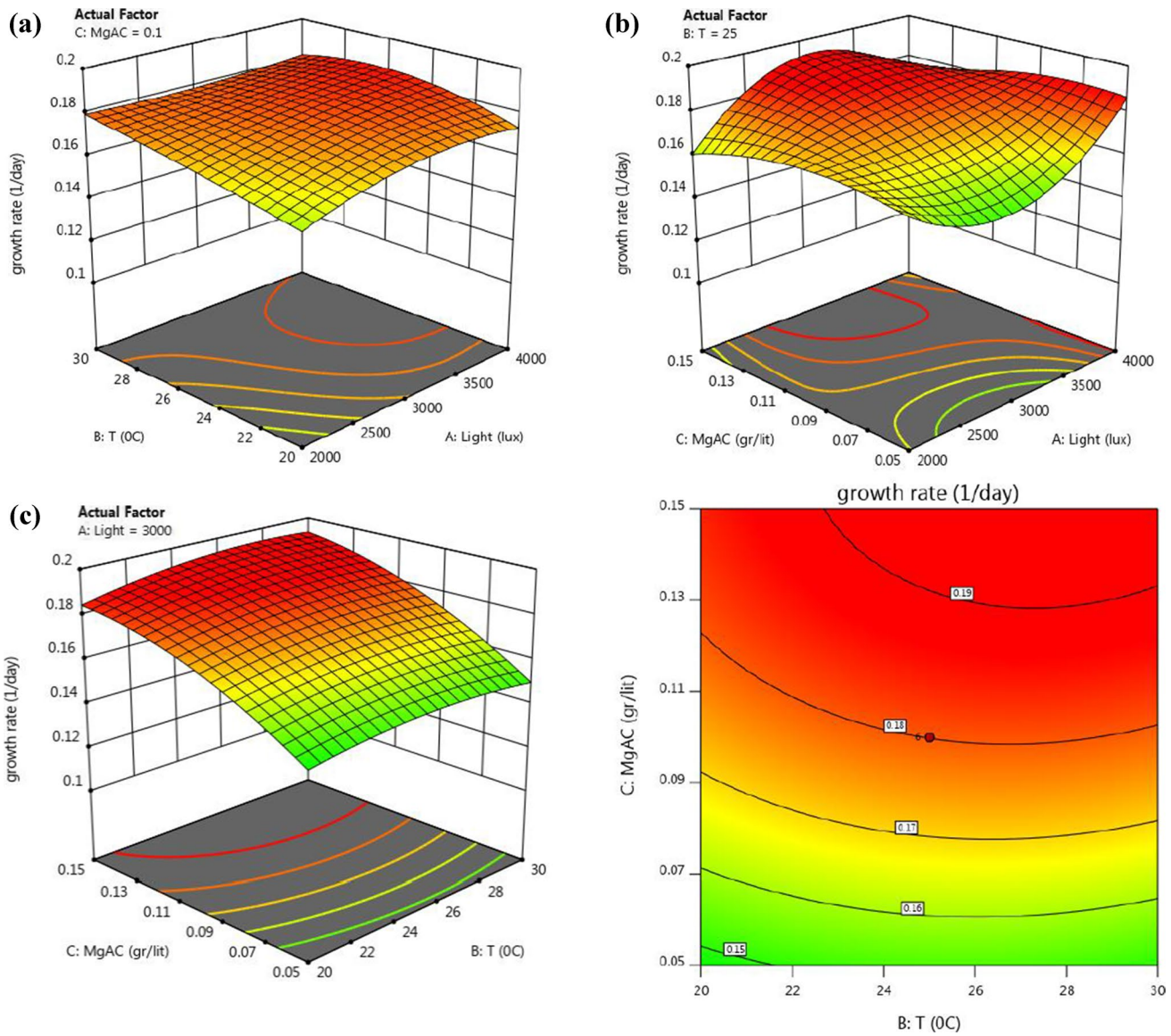

Fig. 6 Surface response scheme (3D)—considerable interaction between input changings and growth rate responses for *C.S. PA.91*. **a** Interaction between light intensity and temperature; **b** interaction between light intensity and MgAC-NPs; **c** interaction between temperature and MgAC-NPs on growth rate responses

C.S. PA.91 in wastewater, there is no study in writing on the effect of light on MgAC-NPs on microalgae growth. Therefore, it is necessary to assess the performance of MgAC in processing urban wastewater under different light intensities. Growth increases with increased light intensity. Specific light intensity and the cycle of light/darkness are required to obtain microalgae photosynthesis. The composition of the energy molecule (ATP and NADPH) to start at the dark photosynthetic responses is needed for carbon assimilation (Villanova and Spetea 2021). The growth rate and biomass yield and wastewater treatment depend on the penetration of light and temperature conditions (Ferro et al. 2018). In this discussion, ANOVA has vouched for a significant permeation on light intensity in biomass production (Table 4). The optimum growth of *C.S. PA.91* under 37 μmol m^{-2} s^{-1} intensity for a light/dark course of 12 h was obtained. The culture was incubated at the concentration of MgAC-NPs 0.1 g L^{-1} for a temperature of 25 ℃, and the intensity of light μmol m^{-2} s^{-1} has enhancement stress, leading to increased growth and biomass yield, as presented in Figs. 5, 6, 7, and 8a, b. The light intensity > 55.5 μmol m^{-2} s^{-1} has increased the microalgae growth and pigment contents but decreased at severities > 111 μmol m^{-2} s^{-1} due to photoinhibition. Also, when the culture is stored under optimal light conditions (18.5 μmol m^{-2} s^{-1}), *C.S. PA.91* has shown fewer CDW

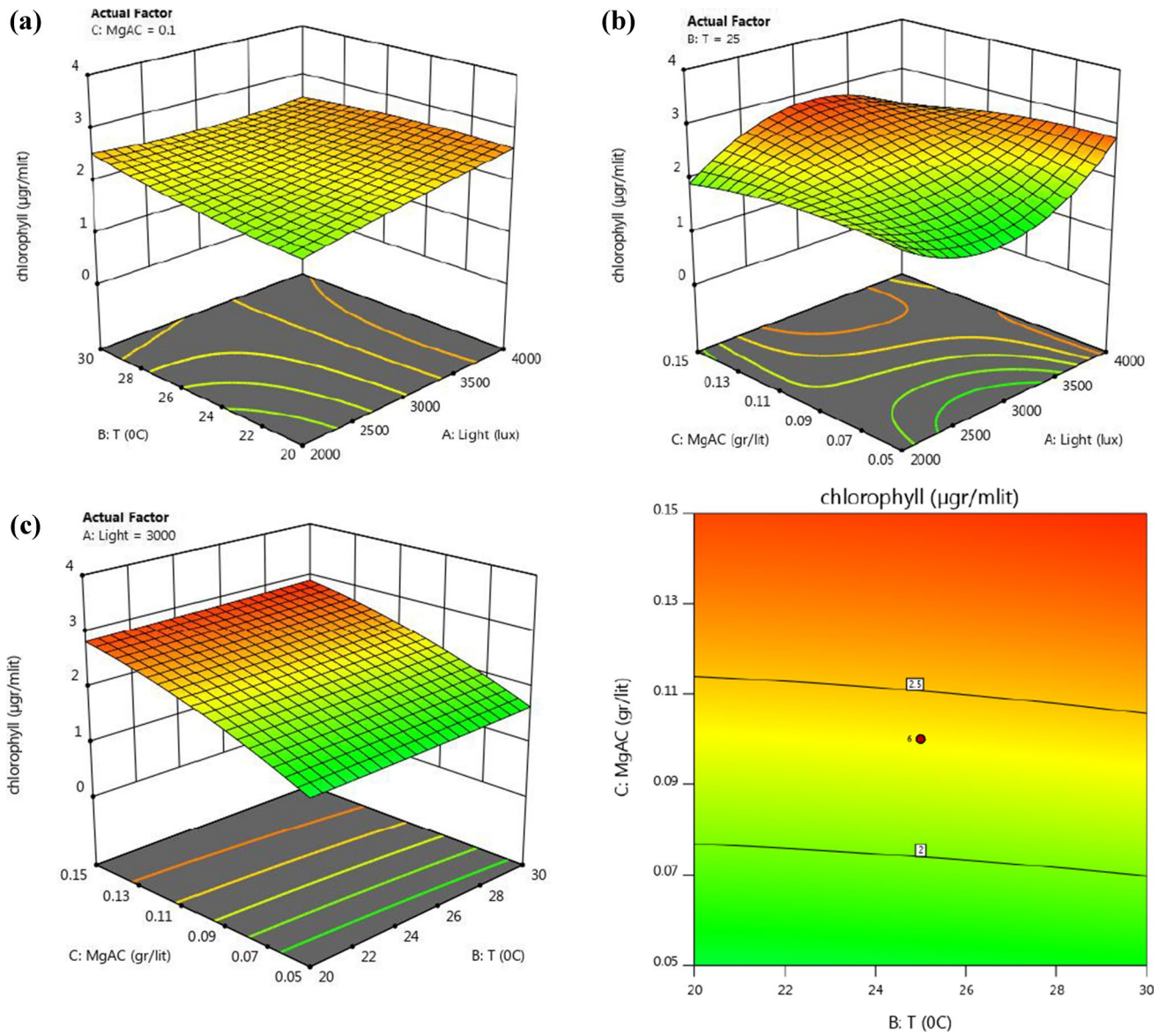

Fig. 7 Surface response scheme (3D)—considerable interaction between input changings and chlorophyll responses for *C.S. PA.91*. **a** Interaction between light intensity and temperature; **b** interaction between light intensity and MgAC-NPs; **c** interaction between temperature and MgAC-NPs on chlorophyll responses

(0.25 mg mL^{-1}), slower growth rate (0.12 day^{-1}), and less chlorophyll and carotenoid (2.08 and 0.15 µg mL^{-1}) but for the concentration MgAC-NPs 0.05 g L^{-1} and 20 ℃, it has shown increased CDW (0.46 mg mL^{-1}), increased growth rate (0.19 day^{-1}), and increased chlorophyll and carotenoid (3.68 and 0.27 µg mL^{-1}) at light 37 µmol m^{-2} s^{-1} presentation condition. Essentially, the optimal condition for DW and μ may be the same (as also implied from Figs. 5 and 6). Physiological or internal acclimatization of microalgae to light intensity is achieved by various mechanisms, such as the type of pigment, the rate of dark respiration, and the presence of essential fatty acids. Simultaneously, morphological photoclimation occurs with changes in cell congestion or volume, density, and some photosynthetic equipment, namely, thylakoid membrane. Furthermore, it is stated that algae exceed the intensity of low light (boundaries) through the desaturation of the chloroplast membrane (Babaei et al. 2020).

The inhibition of growth or photoinhibition affected by the overhead light on the impregnation point was probably owing to the loss of the photosynthetic receiver system in the chloroplast (Manoj and Manekkathodi 2021). Nevertheless, it may be compensated by disclosing the microalgae cells for short courses of light periods. Extending the light period can increase microalgae growth if the light is limited. Howsoever the problem, the amount of light

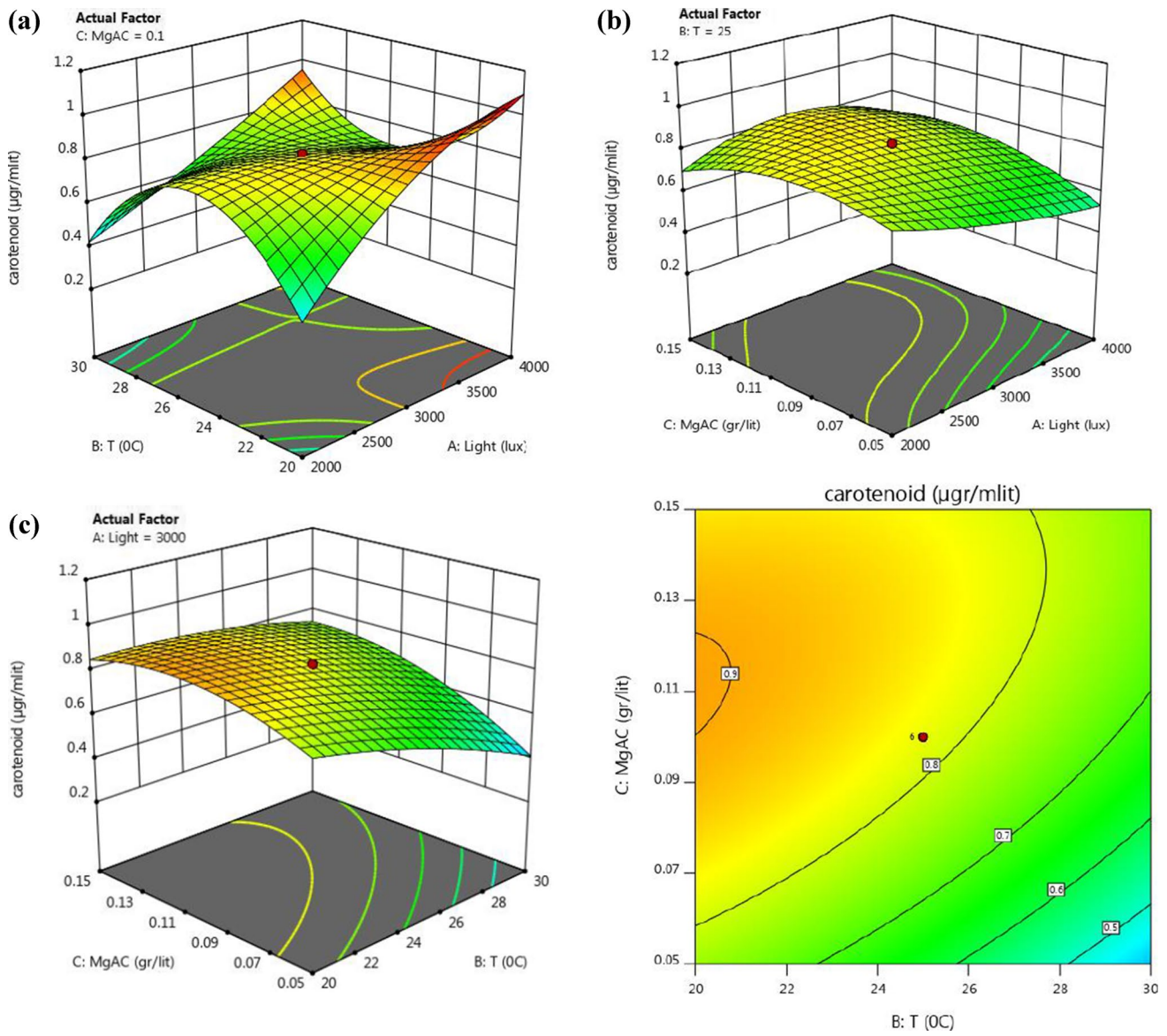

Fig. 8 Surface response scheme (3D)—considerable interaction between input changings and carotenoid responses for *C.S. PA.91*. **a** Interaction between light intensity and temperature; **b** interaction between light intensity and MgAC-NPs; **c** interaction between temperature and MgAC-NPs on carotenoid responses

attained by microalgae depends primarily on the reactor design (Inostroza et al. 2021). The physiological or internal conformity of microalgae with light intensity has arrived at various mechanisms, such as types of pigments, dark breathing rates, and the presence of essential fatty acids. At the same time, morphological photo acclimation occurs with changes in cell density or volume density and the number of photosynthetic equipment, namely the thylakoid membrane (Nzayisenga et al. 2020). Exposure to high light intensity increases its extracellular polysaccharide content. As a rule, microalgae biomass production improves with an increase in light intensity below the optimal value. At the same time, it decreases at the intensity of light exceeding the optimal value due to damage to the photocell system. In addition, it is indicated that algae exceed the intensity of low light (limits) by detecting chloroplast membranes (Deng et al. 2018).

Carbon produced via photosynthesis is required to synthesize lipids until microalgae are stored in excellent lighting conditions (Xue et al. 2020). The center of the reaction is more responsible for damage during an increase in light exposure. In particular, photosynthesis and heterotrophy can coordinate the energy and metabolism of carbon at the cell level below mixotrophy. However, the path that underlies the proportion between two metabolic operations is still obscure, and several studies have been performed on the effects of

light intensity on this synergy (Babaei et al. 2020). Light intensity is an essential factor for regulating microalgae growth and biomass production. This confirms that mixotrophic cultivation is more practical for microalgae biomass production because nutrients can be used with mixotrophic culture, catering to mediums and energy rather than building the microalgae cells (Ghosh et al. 2021; Marella et al. 2021). Furthermore, it is confirmed that microalgae growth is proportionate to the CO_2 fixation level (Xu et al. 2019; Chen et al. 2020; Zeng et al. 2021). Therefore, it can be recommended that the intensity of light less than 111 µmol m^{-2} s^{-1} is more beneficial for CO_2 fixation and, as a result, for the growth of *C.S. PA.91*. This study's results are constant with prior studies, achieving higher microalgae growth below the higher light intensity.

Temperature

In general, temperature is the most critical extrinsic factor in microalgae cultures, affecting microalgae metabolism and the functioning of photosynthetic and metabolic enzymes, cell growth rate, and biomass composition (Yarkent et al. 2020). ANOVA statistics from this study, *F* value, and *P* value shown in Table 4 have appointed a considerable effect of powerful temperatures in the biomass results in the given range. Notably, the ideal temperature for microalgae growth is the range of temperatures of 20–35 °C. In general, an increase in optimum temperature improves the production of biomass microalgae, while increasing the temperature at the optimal level delays the subsequent growth and resulting the death of microalga cells (Brindhadevi et al. 2021). Temperature responses are often specific to the different species (Saranya and Shanthakumar 2020). In this study, *C.S. PA.91* presented its optimal growth rate and biomass yield at 20 °C. This is a valuable result that means the MgAC-NPs have lowered photosynthetic reaction at a comparatively lower temperature than other species, as presented in response plans Figs. 5, 6, 7, and 8a–c; enhancements in the temperature to 20–30 °C have exponentially enhanced the dry weight of cells, growth rates, and chlorophyll but have decreased carotenoids. Also, under 20 °C or up 35 °C, the temperature retardation or even detention of the growth of microalgae and actuality, for example, at 15 °C, light intensity 55.5 µmol m^{-2} s^{-1} and MgAC-NPs at concentration 0.1 g L^{-1}, the dry weight of cells, growth rates, chlorophyll, and carotenoids were 0.314 mg mL^{-1}, 0.153 day^{-1}, 2.151 and 0.928 µg mL^{-1} respectively. While at 25 °C, the dry weight of cells, growth rates, chlorophyll, and carotenoids were 0.448 mg mL^{-1}, 0.178 day^{-1}, 2.317, and 0.830 µg mL^{-1}, respectively. The results show that *C.S. PA.91* has a good temperature tolerance and seems suitable for outdoor cultivation. This indicates decreased photosynthetic activity in non-optimal conditions.

On the other hand, high temperatures stop the protein of photosynthesis membranes, resulting in decreased photosynthesis and disorders in the smoothness of cells, sizes, and breathing; as a mechanism of self-protection, microalgae synthesis of lipids and several secondary metabolites (antioxidants) to guarantee registers and cell liquidity to some temperature (Nawkarkar et al. 2019). Therefore, higher optimum room temperature stimulates the production of high-quality biodiesel and quantity due to a high total performance of lipids and saturated fatty acids (Yadav et al. 2021). The range of low temperatures commonly efficacy the activity of microalgal photosynthesis by decreasing carbon assimilation. The relationship between critical nutrients weakens, resulting in limited growth and biomass performance (Kainthola et al. 2019). The temperature changes the physiological process of strains by increasing or reducing the rate of biochemical reactions in the cellular compartment. Physiological changes in microalgae will finally have consequences for all ecosystems (Schulze et al. 2019).

Certain microalgae in low light and temperatures (less < than 6 °C) can reproduce on the glacial surface of the Antarctic, so they tend to collect significant amounts of intracellular lipids (Morales-Sánchez et al. 2020). In this study, polar microalgae adapted to cold, such as *C.S.* PA.91, are effective for producing cell dry microalgae and metabolites in cool climates. Therefore, we optimized the cultivation of *C.S. PA.91* at low temperatures. Our results demonstrate that the growth of biomass obtained from *C.S. PA.91* is comparable in certain respects to biomass fertilities of mesophilic microalgae, and another microalga adapted to cold (Schulze et al. 2019; Liu 2020; Cheregi et al. 2021). Furthermore, it is remarkable that the metabolic rate, such as biomass productivity of the polar microalgae and excellent adaptation, is not decreased due to decreased temperatures, as offered by various studies (Saraswati Nayar and Thangavel 2021; Ye et al. 2022).

The photochemical energy process is converted to metabolism in complicated algae cells, where two photosystems (I and II) in thylakoid are responsible for photosynthesis, including taking photos, loading, reducing energy, and water separation. Microalgae have evolved into two physiological adaptations: low-light adaptation with high chlorophyll content and high-light adaptation with low chlorophyll content (da Silva Ferreira and Sant'Anna 2017). Another suggested mechanism involving carotenoids is based on electron transfers from carotenoids to chlorophyll, which is pursued by recombining charges in the primary state (Ravensbergen et al. 2022).

MgAC-NPs

Magnesium amino clay nanoparticles (MgAC-NPs), also identified as 3-aminopropyl magnesium phyllosilicate

(APTES), are functional compounds rich in amine made by APTES and magnesium ions through sol–gel reactions (Khac et al. 2018; Nguyen et al. 2019). Unparalleled physical–chemical nature tends to be pro in the application as a co-additives in the treatment of microalgae (Kim et al. 2016). Elevated delamination levels and short-size diffusion provide precise sheet shapes in a soluble and clear MgAC solution and show doing as a cationic charge block through inimitable interplays of harmful biological molecules (Londono-Calderon et al. 2019). Like other substances containing amines, CO_2 absorption in watery solutions is more efficient and sped up by the presence of MgAC (Nguyen et al. 2021). We apply these MgAC to stimulate CO_2 biofixation of *C.S. PA.91* and lipid production. In addition, MgAC show the ability to create the oxidative stress of the environment and concurrent elective control bacteria in mixotrophic culture.

C.S. PA.91 is cultivated in the attendance of MgAC-NPs in constants from 0 to 0.2 g L^{-1} in conditions determined in "MgAC-based *C.S. PA.91* cultivation and growth media." Growth of *C.S. PA.91* by adding MgAC-NPs under the effect of light and temperature is shown (Figs. 5–8b, c). When *C.S. PA.91* cell growth was approximated based on OD_{680}, the throughout bottom concentrations of MgAC (< 0.2 g L^{-1}) presentation premiere ODs than the control cultivated in the lack of MgAC-NPs. The affirmative effect was apperceived and enhanced with primary contents of MgAC-NPs, peaking at 0.2 g L^{-1}. With much contrast, with higher doses, especially the addition of MgAC 0.5 and 1.0 g L^{-1}, growth slightly decreases compared to that of the control. The cell dry weight of *C.S. PA.91* cultures was increased and had overtaken the highest value of 0.5038 mg mL^{-1} at the 0.05 g L^{-1} MgAC-NP dose, temperature 20 °C, and light intensity 4000 lx (74 µmol m^{-2} s^{-1}). Also, the growth rate, chlorophyll, and carotenoid were 0.187 day^{-1}, 3.013, and 1.001 µg mL^{-1} in the above conditions. With increasing MgAC (1 g L^{-1}), dry cell weight, growth rate, chlorophyll, and carotenoid were scarcely reduced to control ($P > 0.05$). The low contents (< 0.2 g L^{-1}) of MgAC-NPs conclusion in finer microalgae cell growth than in the non-NPs case. These results displayed that the abilities of MgAC-NPs will ameliorate the growth of microalgae cells under specific culture conditions or negatively impact growth in high contents (particularly in 1 g L^{-1}). In treated cells, chlorophyll increases with 0.1 to 0.15 g L^{-1} MgAC-NPs, and this can be a sign of a physiological response to reduce the impact of nanoparticles on algae culture. On the other hand, mgAC-NP high concentrations can significantly suppress cell growth, showing a very toxic effect on cell growth. This parameter reflects the physiological state of the whole algae cell. Microalgae images show that MgAC-NPs are surrounded by microalgae cells in the set because of the instability of the walls affected by the MgAC-NPs group (Kim et al. 2020). Electrostatic interactions and MgAC-NP coagulation mechanisms are expressed through zeta potential. Exposure of microalgae to MgAC-NPs in high contents induces physiological responses through reducing chlorophyll content due to damage to the structure of the pigment, damage to the chloroplast ribosome, inhibition in the electron transport chain in the donor center, increased chlorophyllase activity, blocking chlorophyll synthesis, and reducing the pigment complex. The protein and free radical production that induces the formation of reactive oxygen species, which leads to a decrease in the photosynthesis II system activity 2, is reported (Farooq et al. 2016).

Change of design parameters under optimal and actual conditions

These results indicated that MgAC-NPs could grow *C.S. pa.91* under mixotrophic conditions, but high doses of MgAC-NPs, significantly more than 0.5 g L^{-1}, negatively affect their metabolic activities. Due to the simultaneous positive effect of magnesium amino clay and temperature on microalgae growth, it is possible to compensate for the lack of light at certain hours of the day by nanomaterials, so it is suggested that the lighting hours be reduced from 12 to 9 h. The intensity of light and the characteristic of the wavelength significantly affect the photosynthesis of microalgae. According to the obtained results, the amino-magnesium nanomaterial increases the power of light absorption in the culture medium due to the presence of silica materials in its outer layers. This has a direct effect on microalgae growth. Two completely different ways can disrupt the cell wall through the electrostatic appeal between the positive charge and the negatively charged biomolecules of the cell wall. For example, 50 mg L^{-1} of MgAC-NPs has no harmful effect on the microalgae species *Nan-nochloropsis* sp. (Lee et al. 2013). In addition, MgAC-NPs did not or only softly affected other organisms containing *zooplankton* at concentrations under 100 mg L^{-1} (Lee et al. 2014).

The optimal conditions obtained from the analysis were light intensity of 37 µmol m^{-2} s^{-1}, the temperature of 20 °C, and the nanomaterial content of 0.05 g L^{-1}. The experiment was conducted to determine the dry biomass weight, specific growth rate, chlorophyll, and carotenoids under optimal conditions. In these conditions, dry biomass weight, specific growth rate, chlorophyll, and carotenoid were 3.143 g L^{-1}, 0.152 daily, 2.219, 0.517, and 0.86 µg mL^{-1}, respectively. Also, the present research setup, in natural sewage (Fig. 9). RSM, Optimized, WW, AWW, and WW + MgAC-NPs were expressed as optimized conditions suggested by the Design Expert program: re-doing the experiment under the proposed optimal conditions in autoclaved wastewater, conducting experiments in real wastewater without MgAC nanomaterials, conducting experiments in autoclaved wastewater without MgAC nanomaterials and time, and conducting experiments in real wastewater with MgAC nanomaterials, respectively.

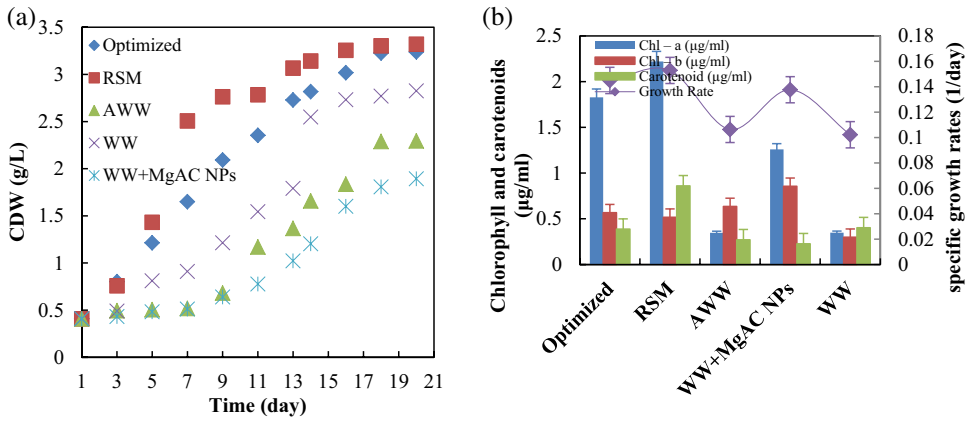

Fig. 9 Parameters change under optimal and real conditions. **a** Cell dry weight; **b** chlorophyll, carotenoids, and specific growth rates

Activities show that they are dissolved and transparent as cationic charge blocks through notable interactions with dangerous biological molecules (Fu et al. 2017). Like other substances containing amines, CO_2 absorption in water solutions is more efficiently sped up by the presence of MgAC-NPs (Fu et al. 2017; Rosa et al. 2018; Barati et al. 2021). These functional amine substances stimulate CO_2 fixing and the production of lipids from the strains of green algae *chlorella* (Farooq et al. 2016; Huang and Kim 2016; Rosa et al. 2018; Barati et al. 2021). In addition, MgAC-NPs can create an oxidative stress environment and simultaneously selectively control bacteria in mixotrophic culture (Farooq et al. 2016; Nguyen et al. 2019). It can be noted that a multitude of these discussions uses green algae as raw material for mixotrophic cultivation (Farooq et al. 2016; Huang and Kim 2016; Rosa et al. 2018; Barati et al. 2021). However, MgAC's bio toxicity on organisms is also recommended and depends on the species and cultural conditions (Kim et al. 2020; Nguyen et al. 2020a; Aslam et al. 2021).

The concentration of MgAC in the supernatant after harvesting the first reused culture media was very little (Nguyen et al. 2020b). Also, environmental effects due to the gradual alteration and inactivation (inert) of the active sites of MgAC over time can be ignored (Calatrava et al. 2019). The inhibition of bacteria and fungi by MgAC is also likely to back the growth of algal granulations and recycled cells (Farooq et al. 2016). In addition, after the agglomeration process, MgAC can also be washed out of the flux by water or return to its precipitate form due to the flexible solubility of water (Khac et al. 2018). We found CDW, chlorophyll, carotenoid, and specific growth rate concentration to be significantly higher in cultures where the AWW + MgAC-NPs (Optimized) concentration was kept at 0.05 g L^{-1}; this shows microalgae to be more sensitive to MgAC-NP inhibition than currently thought. MgAC-NPs will lead to better microalgae growth by creating a stressful environment and absorbing light and carbon dioxide faster.

Lipid

Lipid content is the first response to environmental change conditions and modifying the appropriate cell's physiological state (Redón et al. 2011). Because of ease of cultivation, abundant nutrition, and other added valuable substances, microalgae have been sought as an excellent source of many valuable byproducts such as lipids, protein, carbohydrates, carotenoids, and chlorophyll used broadly in the industrial part (Sarkar et al. 2020; Nguyen et al. 2021). The biomass yield and lipid synthesis of *C.S. PA.91* isolated microalgae were explored in a wastewater medium. At the 0, 0.25, 0.5, 0.75, and 1 g L^{-1} MgAC-NP concentrations, 33.67%, 35.9%, 45.1%, 41.34%, and 38.12% lipid contents are shown (Fig. 11). The contents of the lipids depend highly on many factors, such as species, growth conditions, and growth phase (Seo et al. 2016). At the MgAC-NPs of 0.25 g L^{-1}, *C.S. PA.91* attained the highest dry cell weight of 2.835 g L^{-1} on the 14th day of culture (Fig. 10a). Growth *C.S. PA.91* is also discussed by measuring specific growth rates (μ) d $^{-1}$ microalgae. The specific growth rates were found to be 0.14, 0.149, 0.15, 0.105, and 0.053 day^{-1} in 0, 0.25, 0.5, 0.75, and 1 g L^{-1} MgAC-NP concentrations, respectively. *C.S. PA.91* is also studied for lipid synthesis, as shown in Fig. 10b.

The maximum lipid generation is received at 1.36 g L^{-1} and 45.1% lipid content. Previous reports show that lipid production in microalgae can be motivated by factors such as growth media composition, pH, temperature, illumination of light, and culture (Khanra et al. 2020). Average values vary from 20 to 70% of dry cell weight (Mathimani et al. 2021). Microalgae that toil from poor conditions can hoard a more high percentage of lipids and are valued as renewable energy resources (Ibrahim et al. 2018). However, the potential accumulation of lipids is species specific. Therefore, increased accumulation of lipids is expected for *C.S. PA.91*. In certain stress conditions, algae cells vary their biochemical composition. They can tend to

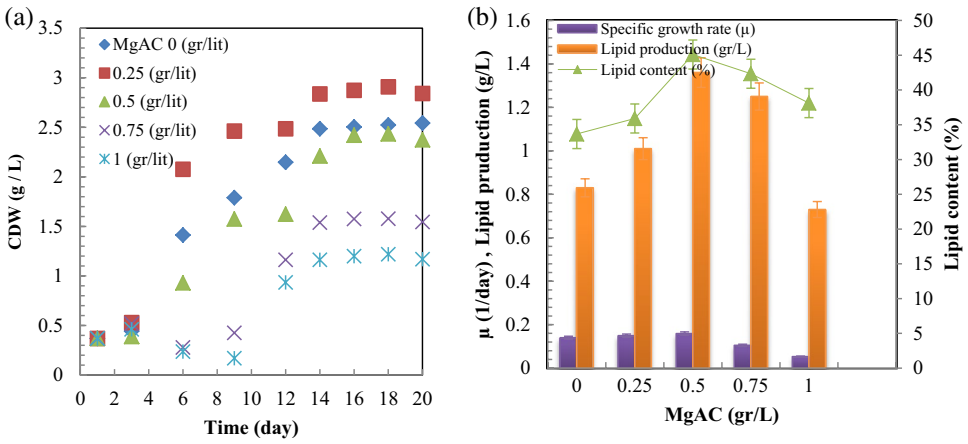

Fig. 10 Relative growth and lipid contraction analysis of *C.S. PA.91*. **a** Growth curve in wastewater medium. **b** Specific growth rate (μ), lipid production, and lipid content

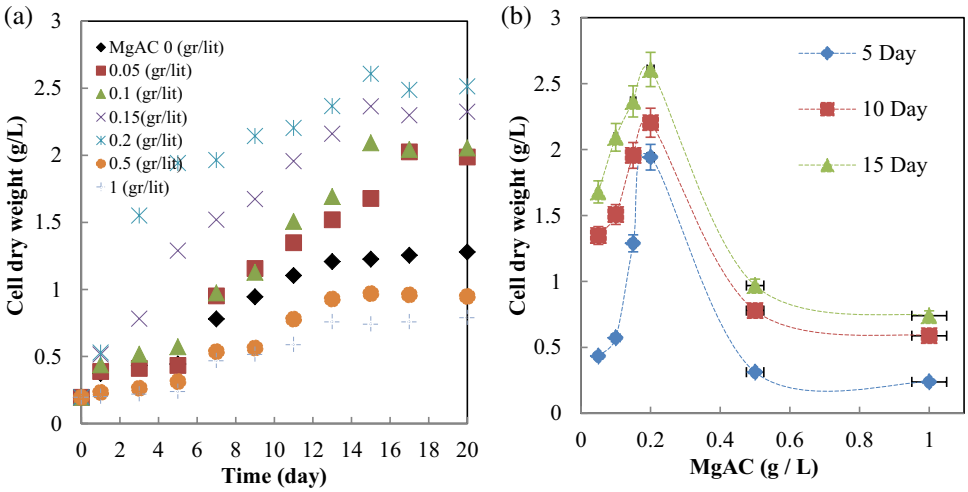

Fig. 11 The effect of MgAC-NPs on the growth of microalgae in real wastewater. **a** Dry weight of biomass, **b** comparison of the dry weight of biomass at different times

adjust cellular metabolism and store larger molecules such as protein and lipids as physiological responses to excluding toxic molecules from the central metabolic pathway (Vasistha et al. 2020). The accumulation of storage compounds in microalgae shows they face a physiologically challenging situation.

Also, MgAC-NPs (high 1 g L^{-1}) did not enhance lipid content or production in contrast to the control. MgAC-NP is explained to force the production of intracellular ROS in microalgae (Bui et al. 2018; Nguyen et al. 2021). Therefore, the extract of pigment and lipids can be a protection mechanism that allows algae cells to overcome oxidative reactions (Ren et al. 2020; Nashmin Elyasi et al. 2021). Nevertheless, to characterize the suitable mechanism that underlies MgAC in *C.S. PA.91*, along with the description of ROS, general research importing genomic, proteomic, and lipidomic analysis is needed. This will be the topic of significant research. Also, their production of an oxidative stress environment can motivate lipid accumulation in microalgae. Nevertheless, their ammonium characteristics can interrupt cell walls and inhibit microbial growth, chiefly at high concentrations. However, it must be reported that factors such as species, dosages, and cultural conditions significantly affect the effects of this aminoclay on organisms(Farooq et al. 2016; Nguyen et al. 2021).

The effect of MgAC-NPs on the growth of microalgae in real wastewater

It should be noted that considering the final target of microalgae cultivation on a large scale, such as wastewater treatment, evaluated MgAC-NP performance is based on natural wastewater rather than artificial. Therefore, we assessed the effect of MgAC-NP concentrations in the growth of *C.S. PA.91* on natural wastewater. *C.S. PA.91* was cultivated in front of the MgAC-NPs at various contents (0–1.0 g L^{-1}) on real wastewater. The growth profile of *C.S. PA.91* with adding MgAC-NPs is shown (Fig. 11a). The positive effect was apperceived and enhanced with the primary contents of MgAC-NPs (0–0.2 g L^{-1}), culminating at 0.2 g L^{-1}. Growth

has declined by MgAC-NPs, adding 0.5 g L^{-1} next. Also, from the 7th day, a 1.0 g L^{-1} test of MgAC-NP presentation significantly had less CDW (P value < 0.05) than all other conditions. The low dose of MgAC-NPs (0.05–0.2 g L^{-1}) shows a higher CDW value than the absence of MgAC-NPs. Cell dry weight *C.S. PA.91* culture enhancement reached the highest 2.607 g L^{-1} at the 0.2 g L^{-1} MgAC-NPs doses. Low doses of MgAC-NPs led to better cellular growth than in the control case (Fig. 11b). However, the presence of MgAC-NPs at higher concentrations (0.5–1.0 g L^{-1}) deterred cell growth at the conception of day 7 (P value > 0.05). These results have shown that the MgAC-NP capacities either improve microalgae cells' growth under specified cultivation conditions or negatively affect growth at high concentrations. MgAC's amino functional groups have acted as biological agents. The cellular activities are affected by the electrostatic interaction between the negatively charged cellular wall of microalgae and the positive load of the MgAC-NPs (Nguyen et al. 2020a).

The MgAC-NP component can result in microbial growth with two throughout different lines. First, a biocidal factor can interfere with stable cellular walls through electrostatic attraction between a bio-molecular applicable positive charge and cell-negative walls (Kim et al. 2016). Neutralization of loads and electrostatic interactions occurs between microalgae cells loaded negatively (–COOH and –NH3) and MgAC-NPs positively charged. Secondly, as a growth advocate, the amine MgAC-NP component can react with CO_2 and speed up the transformation to HCO_3^-, so the enhancement of the dissolved inorganic carbon (DIC) content; Later, it can be recognized for the growth of microalgae photosynthesis (Barati et al. 2021). Due to the presence of silicon plates in the MgAC-NPs structure, better light absorption occurs, so the critical role of MgAC is in enhancing the growth of microalgae and the optical properties of nanoparticles (Pham et al. 2021). By using MgAC-NPs in small amounts, in addition to increasing the growth rate, we obtained wastewater treatment and increased microalgae lipids. In addition, by using nanomaterials and reducing the temperature and light intensity, we also saved energy.

MgAC-microalgae technology for wastewater treatment on a large scale represents an economical and environment-friendly route, but there is a shortage of literature that systematically investigates this technique. This technology helps bio-fixation of CO_2 from the environment and reduces pollution. Also, MgAC-microalgae wastewater bioremediation reduces the discharge of wastewater into water bodies and cleans the environment. The coupling of MgAC-microalgae technology to remove nutrients from wastewater and biofuel generation could be an essential techno-economic strategy for reducing the cost of biofuel production. MgAC-microalgae technology protects socio-economic advancement and holds a better environment. Further, MgAC-microalgae technology has many benefits: (i) the choice of high biomass generation for the recycling of byproducts; (ii) the use of wastewater and MgAC for agriculture, which reduces agricultural costs and removes pollution from the environment; (iii) sewage recycling, which reduces total operating costs; and (iv) the use of MgAC-NPs reduces the cost of the collection system and reduces the main drawback of the microalgae biorefining system, (v) reduces energy use by considering the usable cost of wastewater treatment; wet microalgae biomass is selected over dry biomass, which skips drying and dewatering steps.

Removal of COD by C.S. Pa.91

Figure 12a compares the COD reduction percentage under different operating conditions of adding MgAC-NPs by the native *C.S. PA.91* microalgae of the Sari treatment plant. Fourteen days after the culture of *C.S. PA.91* in wastewater, the COD concentration in MgAC-NPs in several contents

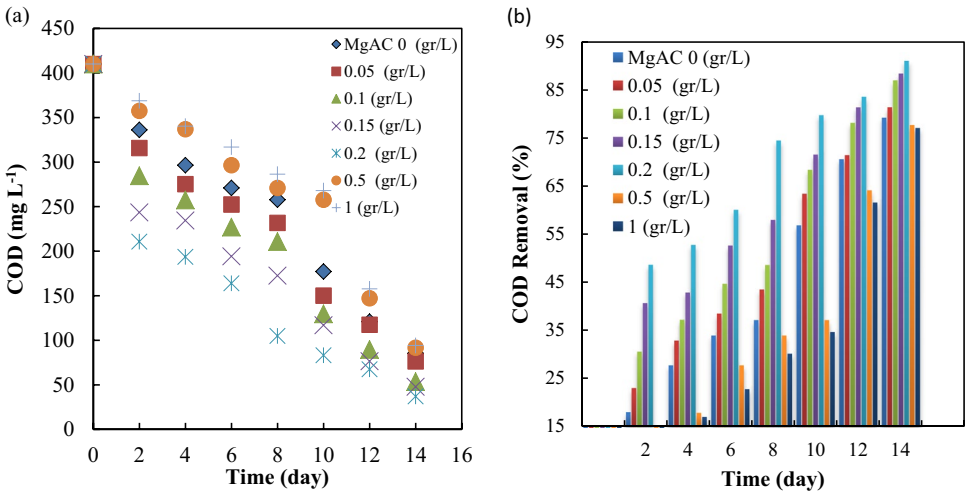

Fig. 12 Removal of COD by *C.S. PA.91* in different amounts of MgAC-NPs. **a** COD removal percentage; **b** COD

(0, 0.05, 0.1, 0.15, 0.2, 0.5, and 1.0 g L^{-1}), respectively, was about 85.27, 76.34, 53.61, 47.8, 36.89, 91.57, and 94.12 mg L^{-1}. Also, the efficiency of COD removal was observed in various MgAC-NP numbers equal to 79.2%, 81.38%, 86.92%, 88.92%, 88.34%, 91.1%, 77.6%, and 77.04% (Fig. 12b). Because of the highest microalgae biomass production of 0.2 g L^{-1} of the MgAC-NPs, it obtained the highest COD removal efficiency (91.1%). The introduction of oxygen into the culture medium donates to organic matter oxidation, with the aeration of cultural values higher than the growth of algae biomass obtained due to the enhancement activity of microalgae photosynthesis (Zhou et al. 2017). Therefore, more oxygen is produced, which helps decrease COD and makes care more effective. It should be an explanation that about half of the biomass microalgae is constructed from carbon. Thus, microalgae use carbon in the culture medium to encounter their needs. Here, too, microalgae have been able to compile a large amount of carbon from the medium and, as a result, have successfully treated this waste (Asadi et al. 2019). The COD removal mechanism depends on the adsorption rate of organic compounds in wastewater by biochar as an ion exchange process (Arun et al. 2020).

The pH of the culture medium decreased to about 8.6 after increasing in the logarithmic phase and then stabilized. Carbon is the primary nutrient for the growth of microalgae cells, directly affects the pH of the culture medium, and is another critical parameter for the growth of microalgae (Kupriyanova and Samylina 2015). Therefore, a proper understanding of the relationship between pH and carbon concentration in the environment and between growth rate and these two parameters is essential. Among the causes of increasing pH in the environment, we can mention the consumption of nitrate by microalgae and the production of OH–, as well as the consumption of CO_2 in the environment by microalgae (Fu et al. 2021). Microalgae in the presence of magnesium amino-clay nanomaterial and quick and easy absorption of carbon dioxide have increased the growth and production of biomass and finally increased the production of microalgae pigments. Due to the presence of amine-containing substances such as monoethanolamide (MEA), the absorption of CO_2 in an aqueous solution is more effectively accelerated by the presence of MgAC. These substances have an amine function to stimulate CO_2 fixation and lipid production in microalgae (Nguyen et al. 2020b). As a growth promoter, MgAC can improve microalgae photosynthesis by accelerating the conversion of CO_2 to bicarbonate (Farooq et al. 2016).

Practical implication and future prospect

Microalgae cultivation has been captivated by microalgae's capability to collect byproducts and produce biofuels. Therefore, increasing commercial and economic potential, high output, sustainability, and environmental friendliness of green materials and microalgae processes are essential. The new Nano-Bio hybrid process offers potential wastewater treatment uses with sustainable biodiesel production. We are using MgAC-NP as an additive, confirming a new trend of wastewater treatment for COD recovery and better lipid productivity that applies to increased lipid production. The Nano-Bio strategy mentioned above has the potential to open the way for the use of renewable energy sources and can be used for refining wastewater. This study brings a pioneering perspective for the future increase of renewable energy processes. However, this study did examine different parameters from MgAC-NPs for wastewater treatment. Nano-biomaterials were explored specifically for real wastewater. NPs surface area is a significant parameter in the application of the formation of microbial associations. Therefore, more research is required to increase NP surface area, which helps provide more effective wastewater treatment. In addition, it is necessary to conduct further research on the sustainability and economic and environmental aspects of microalgae production. In particular, it is further related to nanotechnology and its applications, the effects of problems such as energy consumption, production costs, results, losses, and performance in the entire biorefinery microalgae process, and the friendliness of the environment.

Conclusion

This study showed that the microalgae *C.S. PA.91* have excellent potential for producing high biomass concentrations under the influence of MgAC-NPs. This study investigated the effects of different concentrations of MgAC-NPs on the growth rate of microalgae, the amount of chlorophyll and carotenoids at various temperatures, and the light intensity and different growth cultures such as BG-11, autoclave, and real wastewater. The results showed that dry biomass weight (0.314 mg mL^{-1}), specific growth rate (0.152 day^{-1}), chlorophyll (1.854 mg g^{-1}), and carotenoids (0.425 mg g^{-1}) under an optimum temperature of 20 °C, a radiation intensity of 2000 lx (equivalent to 37 µmol m^{-2} s^{-1}), and an obtained amount of 0.05 g L^{-1} of MgAC-NPs. Also, the maximum lipid production is obtained at 1.36 g L^{-1}, along with 45.1% lipid content. Furthermore, we received the highest COD removal efficiency in the amount of 0.2 g L^{-1} of the MgAC-NPs (91.1%). Therefore, it is very suitable for the biological treatment of wastewater, and optimization of growth and biomass quality of this type of native microalgae can be done using MgAC-NPs. Therefore, we were producing high biomass concentrations under the influence of MgAC-NPs. Furthermore, by using MgAC-NPs in small amounts, in

addition to increasing the growth rate, we obtained wastewater treatment and increased microalgae lipids. Furthermore, the mechanism for removing COD, pigment production as specific production per cell, and lipid extraction is explained based on physiological characteristics and *C.S. P.A 91*. In addition, by using MgAC-NPs and reducing the temperature and light intensity, we also saved energy.

CRediT author statement

Masoumeh Panbehkarbisheh: conceptualization, methodology, formal analysis, validation, software, writing—original draft. Hassan Amini Rad: supervision and critical revision, resources, data curation, investigation, writing—review and editing.

Supplementary Information The online version contains supplementary material available at https://doi.org/10.1007/s11356-023-25779-y.

Acknowledgements The authors would like to give special thanks to Babol Noshirvani University of Technology (BNUT) for the financial support and for providing experimental equipment for the Ph.D. thesis of Masoumeh Panbehkar Bisheh. This work was supported by the Iran High-Tech Laboratory Network (grant number: LabsNet-124570). Also, this work is financially supported by the "Iran Nanotechnology Innovation Council (INIC)" of the Vice-Presidency for Science and Technology IRAN (Contract No. # 153758).

Author contribution All authors contributed to the study conception and design. The second author and corresponding author, Hasan Amini Rad, is mainly responsible for original draft writing, experiment organization, and data analysis, as well as conclusion summary, field experiments, sample analysis, and data compilation of experimental analysis results. Material preparation, data collection, and analysis were performed by Hasan Amini Rad. The first draft of the manuscript was written by Masoumeh Panbehkar Bisheh, and all authors commented on previous versions of the manuscript. All authors read and approved the final manuscript.

Funding This work was supported by Iran High-Tech Laboratory Network and Iran Nanotechnology Innovation Council (INIC) (grant numbers [124570] and [153758]). Masoumeh Panbehkar Bisheh has received research support from Babol Noshirvani University of Technology (BNUT) for the financial support and providing experimental equipment for Ph.D.

Data availability Some or all data used during the study are available from the corresponding author by request.

Declarations

Ethics approval and consent to participate Not applicable.

Consent for publication Not applicable.

Conflict of interest The authors declare no competing interests.

References

Ahmad A, Banat F, Hasan SW (2021) Algae biotechnology for industrial wastewater treatment, bioenergy production, and high-value bioproducts. Sci Total Environ 806:150585. https://doi.org/10.1016/j.scitotenv.2021.150585

Ahmad S, Kothari R, Shankarayan R, Tyagi VV (2020) Temperature dependent morphological changes on algal growth and cell surface with dairy industry wastewater: an experimental investigation. 3 Biotech 10:1–12. https://doi.org/10.1007/s13205-019-2008-x

Almomani F, Al A, Judd S et al (2019) Impact of CO 2 concentration and ambient conditions on microalgal growth and nutrient removal from wastewater by a photobioreactor. Sci Total Environ 662:662–671. https://doi.org/10.1016/j.scitotenv.2019.01.144

Arun J, Gopinath KP, Vigneshwar SS, Swetha A (2020) Sustainable and eco-friendly approach for phosphorus recovery from wastewater by hydrothermally carbonized microalgae: Study on spent bio-char as fertilizer. J Water Process Eng 38:101567. https://doi.org/10.1016/j.jwpe.2020.101567

Asadi P, Rad HA, Qaderi F (2019) Comparison of Chlorella vulgaris and Chlorella sorokiniana pa. 91 in post treatment of dairy wastewater treatment plant effluents. Environ Sci Pollut Res 26:29473–29489. https://doi.org/10.1007/s11356-019-06051-8. (Short)

Asadi P, Rad HA, Qaderi F (2020) Lipid and biodiesel production by cultivation isolated strain Chlorella sorokiniana pa.91 and Chlorella vulgaris in dairy wastewater treatment plant effluents. J Environ Heal Sci Eng 18:573–585. https://doi.org/10.1007/s40201-020-00483-y

Aslam A, Bahadar A, Liaquat R et al (2021) Algae as an attractive source for cosmetics to counter environmental stress. Sci Total Environ 772:144905. https://doi.org/10.1016/j.scitotenv.2020.144905

Babaei A, Ranglová K, Malapascua JR et al (2020) Photobiochemical changes in Chlorella g120 culture during trophic conversion (metabolic pathway shift) from heterotrophic to phototrophic growth regime. J Appl Phycol 32:2807–2818. https://doi.org/10.1007/s10811-020-02137-wPhotobiochemical

Baird RB, Eaton AD, Rice EW (2017) Standard Methods for the Examination of Water and Wastewater

Barati B, Zeng K, Baeyens J et al (2021) Recent progress in genetically modified microalgae for enhanced carbon dioxide sequestration. Biomass and Bioenergy 145:105927. https://doi.org/10.1016/j.biombioe.2020.105927

Brindhadevi K, Mathimani T, Rene ER et al (2021) Impact of cultivation conditions on the biomass and lipid in microalgae with an emphasis on biodiesel. Fuel 284:119058. https://doi.org/10.1016/j.fuel.2020.119058

Bui VKH, Pham TN, Lee Y-C (2018) One-Pot Synthesis of Magnesium Aminoclay-Iron Oxide Nanocomposites for Improved Photo-Fenton Catalytic Performance. J Nanosci Nanotechnol 19:1069–1073. https://doi.org/10.1166/jnn.2019.15942

Calatrava V, Hom EFY, Llamas Á et al (2019) Nitrogen scavenging from amino acids and peptides in the model alga Chlamydomonas reinhardtii. The role of extracellular L-amino oxidase. Algal Res 38:101395. https://doi.org/10.1016/j.algal.2018.101395

Carneiro M, Cicchi B, Maia IB et al (2020) Effect of temperature on growth, photosynthesis and biochemical composition of Nannochloropsis oceanica, grown outdoors in tubular photobioreactors. Algal Res 49:101923. https://doi.org/10.1016/j.algal.2020.101923

Cezare-gomes EA, Mejia-da-silva LC, Pérez-mora LS (2019) Potential of Microalgae Carotenoids for Industrial Application. Appl Biochem Biotechnol 188:602–634. https://doi.org/10.1007/s12010-018-02945-4. (Potential)

Chen J, Li J, Dong W et al (2018) The potential of microalgae in biodiesel production. Renew Sustain Energy Rev 90:336–346. https://doi.org/10.1016/j.rser.2018.03.073

Chen Y, Xu C, Vaidyanathan S (2020) In fluence of gas management on biochemical conversion of CO2 by microalgae for biofuel production. Appl Energy 261:114420. https://doi.org/10.1016/j.apenergy.2019.114420

Cheregi O, Engelbrektsson J, Andersson MX et al (2021) Marine microalgae for outdoor biomass production—A laboratory study simulating seasonal light and temperature for the west coast of Sweden. Physiol Plant 173:543–554. https://doi.org/10.1111/ppl.13412

Choi H-J (2016) Dairy wastewater treatment using microalgae for potential biodiesel application. Environ Eng Res 21:393–400. https://doi.org/10.4491/eer.2015.151

da Silva Ferreira V, Sant'Anna C, (2017) Impact of culture conditions on the chlorophyll content of microalgae for biotechnological applications. World J Microbiol Biotechnol 33:20. https://doi.org/10.1007/s11274-016-2181-6

Das A, Sahoo RK (2019) The Role of Microalgae in Wastewater Treatment. Nat Singapore Pte Ltd, pp 57–64. https://doi.org/10.1007/978-981-13-1586-2

de Farias Silva CE, Bertucco A (2016) Bioethanol from microalgae and cyanobacteria: A review and technological outlook. Process Biochem 51:1833–1842. https://doi.org/10.1016/j.procbio.2016.02.016

Deng X, Chen B, Xue C et al (2018) Biomass production and biochemical profiles of a freshwater microalga Chlor- ella kessleri in mixotrophic culture: effects of light intensity and photoperio- dicity. Bioresour Technol 18:31559–31561. https://doi.org/10.1016/j.biortech.2018.11.032

Di Caprio F, Altimari P, Pagnanelli F (2019) New strategies enhancing feasibility of microalgal cultivations. Stud Surf Sci Catal 179:287–316. https://doi.org/10.1016/B978-0-444-64337-7.00016-1

Farooq W, Uk H, Suk Y, Lee Y (2016) Chlorella vulgaris cultivation with an additive of magnesium-aminoclay. Algal Res 17:211–216. https://doi.org/10.1016/j.algal.2016.05.004

Ferreira A, Marques P, Ribeiro B et al (2018) Combining biotechnology with circular bioeconomy : From poultry, swine, cattle, brewery, dairy and urban wastewaters to biohydrogen. Environ Res 164:32–38. https://doi.org/10.1016/j.envres.2018.02.007

Ferro L, Gorzsás A, Gentili FG, Funk C (2018) Subarctic microalgal strains treat wastewater and produce biomass at low temperature and short photoperiod. Algal Res35:160–167. https://doi.org/10.1016/j.algal.2018.08.031

Fu L, Datta KKR, Spyrou K et al (2017) Phyllosilicate nanoclay-based aqueous nanoparticle sorbent for CO2 capture at ambient conditions. Appl Mater Today 9:451–455. https://doi.org/10.1016/j.apmt.2017.09.009

Fu Y, Hu F, Li H et al (2021) Application and mechanisms of microalgae harvesting by magnetic nanoparticles (MNPs). Sep Purif Technol 265:1–7. https://doi.org/10.1016/j.seppur.2021.118519

Ganesh Saratale R, Kumar G, Banu R et al (2018) A critical review on anaerobic digestion of microalgae and macroalgae and co-digestion of biomass for enhanced methane generation. Bioresour Technol 262:319–332. https://doi.org/10.1016/j.biortech.2018.03.030

Geada P, Oliveira F, Loureiro L et al (2019) Comparison and optimization of different methods for Microcystis aeruginosa's harvesting and the role of zeta potential on its efficiency. Environ Sci Pollut Res 26:16708–16715. https://doi.org/10.1007/s11356-019-04803-0

Geider R, Roche J La (2002) Redfield revisited: variability of C:N: P in marine microalgae and its biochemical basis. Eur J Phycol Eur J Phycol Br Phycol Soc 371:1–17. https://doi.org/10.1017/S0967026201003456

Ghosh A, Sangtani R, Samadhiya K, Kiran B (2021) Maximizing intrinsic value of microalgae using multi - parameter study : conjoint effect of organic carbon, nitrate, and phosphate supplementation. Clean Technol Environ Policy. https://doi.org/10.1007/s10098-021-02192-y

González-Camejo J, Barat R, Pachés M et al (2018) Wastewater nutrient removal in a mixed microalgae–bacteria culture: effect of light and temperature on the microalgae–bacteria competition. Environ Technol (united Kingdom) 39:503–515. https://doi.org/10.1080/09593330.2017.1305001

Hoseini SJ, Bahrami M, Maddahfar M, Hashemi R (2017) Polymerization of graphene oxide nanosheet by using of aminoclay : Electrocatalytic activity of its platinum nanohybrids. 1–11. https://doi.org/10.1002/aoc.3894

Huang W, Kim J (2016) Bioresource Technology Nickel oxide nanoparticle-based method for simultaneous harvesting and disruption of microalgal cells. Bioresour Technol 218:1290–1293. https://doi.org/10.1016/j.biortech.2016.07.091

Ibrahim MF, Kim SW, Abd-aziz S (2018) Advanced bioprocessing strategies for biobutanol production from biomass. Renew Sustain Energy Rev 91:1192–1204. https://doi.org/10.1016/j.rser.2018.04.060

Inostroza C, Solimeno A, García J et al (2021) Improvement of real-scale raceway bioreactors for microalgae production using Computational Fluid Dynamics (CFD). Algal Res 54:102207. https://doi.org/10.1016/j.algal.2021.102207

Ji H, Uk H, Jin E et al (2016) Efficient harvesting of wet blue-green microalgal biomass by two-aminoclay [AC] -mixture systems. Bioresour Technol 211:313–318. https://doi.org/10.1016/j.biortech.2016.03.111

Kainthola J, Kalamdhad AS, Goud VV (2019) A review on enhanced biogas production from anaerobic digestion of lignocellulosic biomass by different enhancement techniques. Process Biochem 84:81–90. https://doi.org/10.1016/j.procbio.2019.05.023

Khac V, Bui H, Park D, Lee Y (2018) Aminoclays for biological and environmental applications : An updated review. Chem Eng J 336:757–772. https://doi.org/10.1016/j.cej.2017.12.052

Khalili A, Najafpour GD, Amini G, Samkhaniyani F (2015) Influence of nutrients and LED light intensities on biomass production of microalgae Chlorella vulgaris. Biotechnol Bioprocess Eng 20:284–290. https://doi.org/10.1007/s12257-013-0845-8

Khanra A, Vasistha S, Kumar P, Rai MP (2020) Role of C/N ratio on microalgae growth in mixotrophy and incorporation of titanium nanoparticles for cell flocculation and lipid enhancement in economical biodiesel application. 3 Biotech 10:1–12. https://doi.org/10.1007/s13205-020-02323-0

Kim B, Praveenkumar R, Lee J et al (2016) Magnesium aminoclay enhances lipid production of mixotrophic Chlorella sp. KR-1 while reducing bacterial populations. Bioresour Technol 219:608–613. https://doi.org/10.1016/j.biortech.2016.08.034

Kim M, Moon J, Lee Y (2020) Loading effects of low doses of magnesium aminoclay on microalgal Microcystis sp. KW growth, macromolecule productions, and cell harvesting. Biomass Bioenergy 139:105619

Kupriyanova EV, Samylina OS (2015) CO 2 Concentrating Mechanism and Its Traits in Haloalkaliphilic Cyanobacteria. Microbiology 84:112–124. https://doi.org/10.1134/S0026261715010075

Lee W, An S, Choi Y (2021) Ammonia harvesting via membrane gas extraction at moderately alkaline pH: A step toward net-profitable nitrogen recovery from domestic wastewater. Chem Eng J 405:126662. https://doi.org/10.1016/j.cej.2020.126662

Lee Y, Jung SW, Kim Y, Shin H (2013) Utilizing the algicidal activity of aminoclay as a practical treatment for toxic red tides. Sci Rep 3(1):1292. https://doi.org/10.1038/srep01292

Lee Y, Uk H, Lee K et al (2014) Aminoclay-conjugated TiO 2 synthesis for simultaneous harvesting and wet-disruption of oleaginous

Chlorella sp. Chem Eng J 245:143–149. https://doi.org/10.1016/j.cej.2014.02.009
Li J, Qiao S, Tan G et al (2019) A Non-innocent Magnesium Organoclay-Based Drug Vehicle for Improving the Cancer Therapy Effect of Methotrexate. AAPS PharmSciTech 20:309. https://doi.org/10.1208/s12249-019-1456-2
Liu J (2020) Exploiting microalgal competition ability to acquire nitrogen and light. Phycol Res. https://doi.org/10.1111/pre.12441
Liyanaarachchi VC, Premaratne M, Ariyadasa TU et al (2021) Two-stage cultivation of microalgae for production of high-value compounds and biofuels: A review. Algal Res 57:102353. https://doi.org/10.1016/j.algal.2021.102353
Londono-Calderon A, Hossen MM, Palo PE et al (2019) Imaging of Unstained DNA Origami Triangles with Electron Microscopy. Small Methods 3:1–10. https://doi.org/10.1002/smtd.201900393
Lv X, Wang Y, Cai C et al (2018) Spectrochimica Acta Part A : Molecular and Biomolecular Spectroscopy Investigation of gel formation and volatilization of acetate acid in magnesium acetate droplets by the optical tweezers. Spectrochim Acta Part A Mol Biomol Spectrosc 200:179–185. https://doi.org/10.1016/j.saa.2018.04.027
Manoj KM, Manekkathodi A (2021) Light's interaction with pigments in chloroplasts: The murburn perspective. J Photochem Photobiol 5:100015. https://doi.org/10.1016/j.jpap.2020.100015
Marella TK, Bhattacharjya R, Tiwari A (2021) Impact of organic carbon acquisition on growth and functional biomolecule production in diatoms. Microb Cell Fact 20:1–13. https://doi.org/10.1186/s12934-021-01627-x
Mathimani T, Sekar M, Shanmugam S et al (2021) Relative abundance of lipid types among Chlorella sp. and Scenedesmus sp. and ameliorating homogeneous acid catalytic conditions using central composite design (CCD) for maximizing fatty acid methyl ester yield. Sci Total Environ 771:144700. https://doi.org/10.1016/j.scitotenv.2020.144700
Mishra SK, Suh WI, Farooq W et al (2014) Rapid quantification of microalgal lipids in aqueous medium by a simple colorimetric method. Bioresour Technol 155:330–333. https://doi.org/10.1016/j.biortech.2013.12.077
Morales-Sánchez D, Schulze PSC, Kiron V, Wijffels RH (2020) Production of carbohydrates, lipids and polyunsaturated fatty acids (PUFA) by the polar marine microalga Chlamydomonas malina RCC2488. Algal Res 50:102016. https://doi.org/10.1016/j.algal.2020.102016
Nalley JO, O'Donnell DR, Litchman E (2018) Temperature effects on growth rates and fatty acid content in freshwater algae and cyanobacteria. Algal Res 35:500–507. https://doi.org/10.1016/j.algal.2018.09.018
Naseem T, Waseem M (2021) A comprehensive review on the role of some important nanocomposites for antimicrobial and wastewater applications. Int J Environ Sci Technol. https://doi.org/10.1007/s13762-021-03256-8
Nashmin Elyasi S, He L, Tsapekos P et al (2021) Could biological biogas upgrading be a sustainable substitution for water scrubbing technology? A case study in Denmark. Energy Convers Manag 245:14550. https://doi.org/10.1016/j.enconman.2021.114550
Nawkarkar P, Singh AK, Abdin MZ, Kumar S (2019) Life cycle assessment of Chlorella species producing biodiesel and remediating wastewater. J Biosci 44:1–15. https://doi.org/10.1007/s12038-019-9896-0
Nguyen MK, Kim MK, Moon JY et al (2021) Influence of chitosan-based carbon dots added in MgAC-containing culture medium on green alga Tetraselmis sp. J Appl Phycol 33:765–775. https://doi.org/10.1007/s10811-021-02368-5
Nguyen MK, Moon J, Khac V et al (2019) Recent advanced applications of nanomaterials in microalgae biorefinery. Algal Res 41:101522. https://doi.org/10.1016/j.algal.2019.101522
Nguyen MK, Moon J, Lee Y (2020a) Ecotoxicology and Environmental Safety Microalgal ecotoxicity of nanoparticles : An updated review. Ecotoxicol Environ Saf 201:110781. https://doi.org/10.1016/j.ecoenv.2020a.110781
Nguyen MK, Moon J, Lee Y (2020b) Loading effects of low doses of magnesium aminoclay on microalgal Microcystis sp. KW growth, macromolecule productions, and cell harvesting. Biomass and Bioenergy 139:105619. https://doi.org/10.1016/j.biombioe.2020b.105619
Nzayisenga JC, Farge X, Groll SL, Sellstedt A (2020) Effects of light intensity on growth and lipid production in microalgae grown in wastewater. Biotechnol Biofuels 13:1–8. https://doi.org/10.1186/s13068-019-1646-x
Ogbonna JC, Nweze NO, Ogbonna CN (2021) Effects of light on cell growth, chlorophyll, and carotenoid contents of Chlorella sorokiniana and Ankistrodesmus falcatus in poultry dropping medium. J Appl Biol Biotechnol 9:157–163. https://doi.org/10.7324/JABB.2021.9215
Park J, Jeong HJ, Yoon EY, Moon SJ (2016) Easy and rapid quantification of lipid contents of marine dinoflagellates using the sulpho-phospho-vanillin method. Algae 31:391–401. https://doi.org/10.4490/algae.2016.31.12.7
Pham TN, Hue NT, Lee Y et al (2021) RSC Advances PAPER A hybrid design of Ag-decorated ZnO on layered nanomaterials (MgAC) with photocatalytic and. RSC Adv 11:38578–38588. https://doi.org/10.1039/D1RA08365A
Ramlee A, Rasdi WNNW, Wahid MEA, Jusoh M (2021) Microalgae and the Factors Involved in Successful Propagation for Mass Production. J Sustain Sci Manag 16:21–42. https://doi.org/10.46754/JSSM.2021.04.003
Ravensbergen J, Pillai S, Méndez-Hernández DD et al (2022) Dual Singlet Excited-State Quenching Mechanisms in an Artificial Caroteno-Phthalocyanine Light Harvesting Antenna. ACS Phys Chem Au 2:59–67. https://doi.org/10.1021/acsphyschemau.1c00008
Redón M, Guillamón JM, Mas A, Rozès N (2011) Effect of growth temperature on yeast lipid composition and alcoholic fermentation at low temperature. Eur Food Res Technol 232:517–527. https://doi.org/10.1007/s00217-010-1415-3
Ren HY, Dai YQ, Kong F et al (2020) Enhanced microalgal growth and lipid accumulation by addition of different nanoparticles under xenon lamp illumination. Bioresour Technol 297:122409. https://doi.org/10.1016/j.biortech.2019.122409
da Rosa GM, de Morais MG, Costa JAV (2018) Green alga cultivation with monoethanolamine: Evaluation of CO2 fixation and macromolecule production. Bioresour Technol 261:206–212. https://doi.org/10.1016/j.biortech.2018.04.007
Ruan W, Yuan X, Eltzschig HK (2021) Circadian rhythm as a therapeutic target. Nat Rev Drug Discov 20:287–307. https://doi.org/10.1038/s41573-020-00109-w
Saranya D, Shanthakumar S (2020) Effect of culture conditions on biomass yield of acclimatized microalgae in ozone pre-treated tannery effluent: A simultaneous exploration of bioremediation and lipid accumulation potential. J Environ Manage 273:111129. https://doi.org/10.1016/j.jenvman.2020.111129
Saraswati Nayar, Thangavel G (2021) CsubMADS1, a lag phase transcription factor, controls development of polar eukaryotic microalga Coccomyxa subellipsoidea C-169. Plant J 107:1228–1242. https://doi.org/10.1111/tpj.15380
Sarkar S, Manna MS, Bhowmick TK, Gayen K (2020) Extraction of chlorophylls and carotenoids from dry and wet biomass of isolated Chlorella Thermophila: Optimization of process parameters and modelling by artificial neural network. Process Biochem 96:58–72. https://doi.org/10.1016/j.procbio.2020.05.025
Schulze PSC, Hulatt CJ, Morales-Sánchez D et al (2019) Fatty acids and proteins from marine cold adapted microalgae for

biotechnology. Algal Res 42:101604. https://doi.org/10.1016/j.algal.2019.101604

Seo JY, Praveenkumar R, Kim B et al (2016) Downstream integration of microalgae harvesting and cell disruption by means of cationic surfactant-decorated Fe3O4 nanoparticles. Green Chem 18:3981–3989. https://doi.org/10.1039/c6gc00904b

Singh A, Singh NB, Afzal S et al (2018) Zinc oxide nanoparticles: a review of their biological synthesis, antimicrobial activity, uptake, translocation and biotransformation in plants. J Mater Sci 7:909–917. https://doi.org/10.1007/s10853-017-1544-1

Sirajunnisa AR, Surendhiran D (2016) Algae – A quintessential and positive resource of bioethanol production: A comprehensive review. Renew Sustain Energy Rev 66:248–267. https://doi.org/10.1016/j.rser.2016.07.024

Ubando AT, Rivera DRT, Chen WH, Culaba AB (2020) Life cycle assessment of torrefied microalgal biomass using torrefaction severity index with the consideration of up-scaling production. Renew Energy 162:1113–1124. https://doi.org/10.1016/j.renene.2020.08.068

Vasistha S, Khanra A, Rai MP (2020) Influence of microalgae-ZnO nanoparticle association on sewage wastewater towards efficient nutrient removal and improved biodiesel application : An integrated approach. J Water Process Eng 39:101711. https://doi.org/10.1016/j.jwpe.2020.101711

Villanova V, Spetea C (2021) Mixotrophy in diatoms : Molecular mechanism and industrial potential. Physiologia Plantarum 173:603–611. https://doi.org/10.1111/ppl.13471

Visnovitz T, Osteikoetxea X, Sódar BW et al (2019) An improved 96 well plate format lipid quantification assay for standardisation of experiments with extracellular vesicles. J Extracell Vesicles 8:1565263. https://doi.org/10.1080/20013078.2019.1565263

Wang R, Jing G, Zhou X, Lv B (2017) Removal of chromium (VI) from wastewater by Mg-aminoclay coated nanoscale zero-valent iron. J Water Process Eng 18:134–143. https://doi.org/10.1016/j.jwpe.2017.05.013

Xu X, Gu X, Wang Z et al (2019) Progress, challenges and solutions of research on photosynthetic carbon sequestration efficiency of microalgae. Renew Sustain Energy Rev 110:65–82. https://doi.org/10.1016/j.rser.2019.04.050

Xue R, Fu L, Dong S et al (2020) Promoting Chlorella photosynthesis and bioresource production using directionally prepared carbon dots with tunable emission. J Colloid Interface Sci. https://doi.org/10.1016/j.jcis.2020.02.080

Yadav G, Sekar M, Kim S et al (2021) Lipid content, biomass density, fatty acid as selection markers for evaluating the suitability of four fast growing cyanobacterial strains for biodiesel production. Bioresour Technol 325:124654. https://doi.org/10.1016/j.biortech.2020.124654

Yaqoubnejad P, Amini H, Taghavijeloudar M (2021) Development a novel hexagonal airlift flat plate photobioreactor for the improvement of microalgae growth that simultaneously enhance CO 2 biofixation and wastewater treatment. J Environ Manage 298:113482. https://doi.org/10.1016/j.jenvman.2021.113482

Yarkent Ç, Gürlek C, Oncel SS (2020) Potential of microalgal compounds in trending natural cosmetics: A review. Sustain Chem Pharm 17:100304. https://doi.org/10.1016/j.scp.2020.100304

Ye N, Han W, Toseland A (2022) The role of zinc in the adaptive evolution of polar phytoplankton. Nat Ecol Evol. https://doi.org/10.1038/s41559-022-01750-x

Zeng J, Wang Z, Chen G (2021) Biological characteristics of energy conversion in carbon fixation by microalgae. Renew Sustain Energy Rev 152:111661. https://doi.org/10.1016/j.rser.2021.111661

Zhou W, Li Y, Gao Y, Zhao H (2017) Nutrients removal and recovery from saline wastewater by Spirulina platensis. Bioresour Technol 245:10–17. https://doi.org/10.1016/j.biortech.2017.08.160